Polymer 50 (2009) 4407–4423

Contents lists available at ScienceDirect

Polymer

journal homepage: www.elsevier.com/locate/polymer

Feature Article

Atom transfer radical polymerization in inverse miniemulsion: A versatile route toward preparation and functionalization of microgels/nanogels for targeted drug delivery applications

Jung Kwon Oh [a,*], Sidi A. Bencherif [b], Krzysztof Matyjaszewski [b,**]

[a] Dow Chemical Company, Midland, MI 48674, USA
[b] Department of Chemistry, Carnegie Mellon University, 4400 Fifth Avenue, Pittsburgh, PA 15213, USA

ARTICLE INFO

Article history:
Received 29 April 2009
Received in revised form
19 June 2009
Accepted 20 June 2009
Available online 26 June 2009

Keywords:
ATRP
Nanogels
Drug delivery system
Emulsion
Inverse miniemulsion

ABSTRACT

This short review describes application of atom transfer radical polymerization (ATRP) in inverse miniemulsion and disulfide–thiol exchange to prepare well-defined biodegradable functional nanogels (ATRP-nanogels). Due to the formation of uniform network, the ATRP-nanogels have higher swelling ratios, better colloidal stability, and controlled degradation, as compared to nanogels prepared by conventional free-radical polymerization. Various water-soluble biomolecules such as anticancer drugs, carbohydrates, proteins, and star branched polymers were incorporated into ATRP-nanogels at high loading level, by *in-situ* physical loading or by *in-situ* chemical incorporation via covalent bonds. The nanogels crosslinked with disulfide or polyester linkages were degraded either in the presence of biocompatible reducing agents or by hydrolysis for controllable release of the encapsulated drugs. ATRP-nanogels contain bromine end groups that enable further chain extension and functionalization with biorelated molecules. They are also easily functionalized by copolymerization with functional monomers or use of functional ATRP initiator during synthesis. These functional nanogels have capability to be further chemically modified and bioconjugated with cell-targeting proteins, antibodies, and integrin-binding peptides to increase cellular uptake via clathrin-mediated endocytosis. These results suggest that such well-defined functional nanogels have great potential for targeted drug delivery applications.

1. Introduction

Polymer-based drug delivery systems (DDS) have attracted significant attention in biomedicine, pharmaceutics, and bio-nanotechnology. In particular, polymer-based DDS with controllable release of therapeutics and cell targeting have the potential to treat numerous diseases, including cancers, with a reduction in the side effects of the drugs. Several types of polymer-based DDS have been explored and microgels/nanogels are among the most promising DDS. Microgels are a class of small crosslinked hydrogel particles. When the microgel particles are submicron-sized they are known as nanogels. Like hydrogels, microgels/nanogels are three-dimensional biocompatible materials with high water content. In addition, they have tunable size from submicrons to tens of nanometers, a large surface area for multivalent bioconjugation, and an interior network for incorporation of therapeutics [1–3]. Entrapment of biomolecules including anticancer drugs, proteins, carbohydrates, DNA, genes, nucleic acids, and inorganic nanoparticles in microgels/nanogels as well as their *in vitro* release have been already extensively investigated [4–14].

Several criteria, including control over biological, chemical, and physical properties, are required for the design and development of effective microgel/nanogel-based DDS for *in vivo* biomedical applications. They include non-toxicity to cells, stability for prolonged circulation in blood stream, high loading efficiency and controllable release of therapeutics, in addition to functionality for further bioconjugation, dimensional control, and biodegradability. The last criterion modulates the release of therapeutics for a desired period of time as well as enables the removal of the empty device after drug release. A common approach to biodegradability is to introduce (bio)degradable linkages into the microgel/nanogel crosslinked network. The linkages reported in literature include oligolactate esters [15–19], anhydrides [20], peptides [21–24], polyperoxides [25], 1,2-dihydroxyethylenes [26], acetals [27–33], poly(3-hydroxybutyrate) [34], polyphosphoesters [35,36], disulfides [4,37], and hydrazones [38,39]. The resulting crosslinked polymers are degraded to water-soluble polymers in external environments.

* Corresponding author. Tel.: +1 989 638 4617; fax: +1 989 638 9425.
** Corresponding author. Tel.: +1 412 268 3209; fax: +1 412 268 6897.
E-mail addresses: jkoh2@dow.com (J.K. Oh), km3b@andrew.cmu.edu (K. Matyjaszewski).

0032-3861/$ – see front matter © 2009 Elsevier Ltd. All rights reserved.
doi:10.1016/j.polymer.2009.06.045

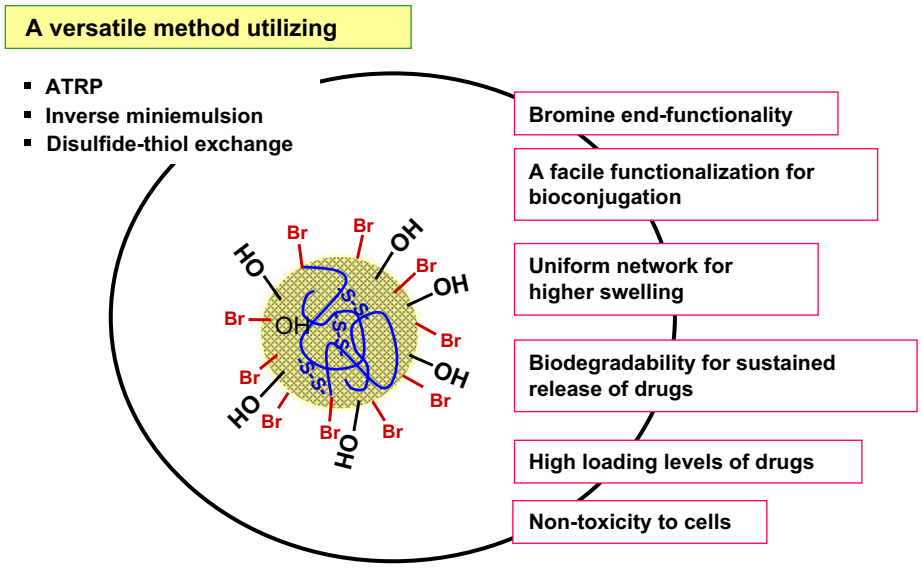

Fig. 1. Illustration of unique features of biodegradable nanogels prepared by atom transfer radical polymerization in inverse miniemulsion of oligo(ethylene glycol) monomethyl methacrylate in the presence of a disulfide-functionalized dimethacrylate.

Microgels/nanogels are prepared by various methods of copolymerization of hydrophilic or water-soluble monomers in the presence of difunctional or multifunctional crosslinkers [4]. They include photolithographic [40], micromolding [41,42], microfluidic [43,44], reverse micellar [45,46], membrane emulsification [47,48], and homogeneous gelation methods [49,50]. They are also prepared by heterogeneous free-radical polymerization in various media including dispersion [51,52], precipitation [53–55], inverse (mini)-emulsion, and inverse microemulsion. However, due to the use of uncontrolled polymerization processes, all of these examples resulted in the preparation of polymers with broad molecular weight distribution (i.e. $M_w/M_n > 2.0$).

Controlled/living radical polymerization (CRP) techniques [56–61] have been explored in various media including water, (inverse) miniemulsion, and dispersion for the preparation of crosslinked particles and gels with well-controlled polymer segments [62–71]. Nevertheless, only a few papers report the use of CRP methods to prepare well-defined microgels/nanogels. Atom transfer radical polymerization (ATRP) [72,73] in water yielded poly(*N*-isopropyl acrylamide) (PNIPAM)-based nanogels with a diameter 67 nm in water at 25 °C [21]. Reversible addition fragmentation transfer (RAFT) polymerization allowed for the preparation of acid-cleavable core-shell nanoparticles [74], poly(vinyl acetate)-based nanogels [75], thermally-responsive [76] and double hydrophilic [77] block copolymer nanogels.

Recently, a versatile method for preparing and functionalizing well-defined biodegradable nanogels for targeted drug delivery applications has been developed [4,78–82]. The method utilizes ATRP [72,73], inverse miniemulsion polymerization [83], and disulfide–thiol exchange [84,85]. The novel approach allows the preparation of biomaterials with many useful predeterminable site-specific features. As illustrated in Fig. 1, the features include uniform network, high loading efficiency, novel distributed functionality including bromine end groups, and degradation by hydrolysis or through a disulfide–thiol exchange. This paper will review the preparation, functionalization, and biomedical applications of well-defined non-crosslinked and crosslinked nanogels of poly(oligo-(ethylene glycol) monomethyl ether methacrylate) (POEOMA) by inverse miniemulsion ATRP.

1.1. Inverse miniemulsion and microemulsion polymerization

Inverse miniemulsion polymerization is a water-in-oil (W/O) heterogeneous polymerization process that forms kinetically stable macroemulsions at, below, or around the critical micellar concentration (CMC). This process contains aqueous droplets (including water-soluble monomers) stably dispersed, with the aid of oil-soluble surfactants, in a continuous organic medium. Stable inverse miniemulsions are formed under high shear by either a homogenizer or a high speed mechanical stirrer. Oil-soluble nonionic surfactants

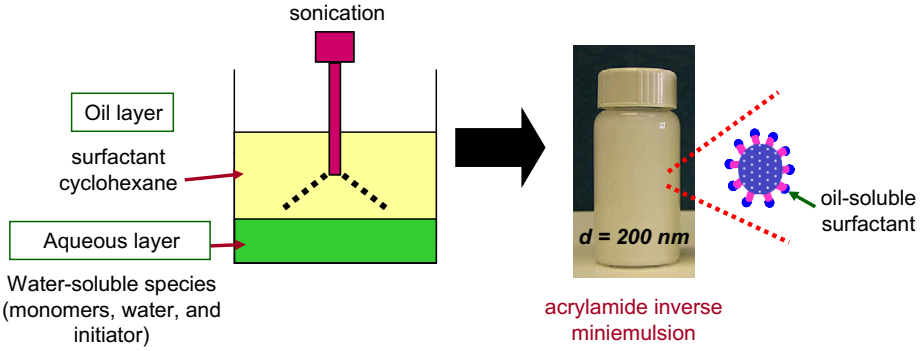

Fig. 2. A schematic representation of inverse miniemulsion or microemulsion polymerization for the preparation of nanometer-sized particles of water-soluble and water-swellable polymers as well as crosslinked particles in the presence of crosslinkers.

with hydrophilic-lipophilic balance (HLB) value around 4 are used to implement colloidal stability of the resulting inverse emulsion. Upon addition of radical initiators, polymerization occurs within the aqueous droplets producing colloidal particles (Fig. 2) [83]. Several reports have demonstrated the preparation of stable particles of hydrophilic and water-soluble polymers [86–89], polyaniline nanoparticles [90], and organic–inorganic hybrid particles [91–93]. This method also allows for the preparation of crosslinked microgels in the presence of difunctional crosslinkers [27,94–100]. In addition, CRP techniques including ATRP [78,79,82,101,102] and RAFT [103] in inverse miniemulsion have been explored to prepare well-defined nanoparticles and nanogels.

Inverse microemulsion polymerization also involves aqueous droplets, stably dispersed with the aid of a large amount of oil-soluble surfactants, above the critical micellar concentration, in a continuous organic medium. Polymerization occurs within the aqueous droplets, producing stable hydrophilic water-soluble colloidal nanoparticles with a diameter of less than 50–100 nm [104,105]. This method has been also explored for the preparation of well-defined nanoparticles [106–111], magnetic polymeric particles [112,113], and nanogels in the presence of difunctional crosslinkers [114–119].

The resulting nanogels by both polymerization methods are produced in the form of dispersions in organic solvents with oil-soluble surfactants. Biomedical applications require removal of residual monomers, oil-soluble surfactants, and organic solvents. Nanogels are then redispersed in water before use. For comparison, aqueous precipitation polymerization of water-soluble monomers in the presence of difunctional crosslinkers is also allowed for the preparation of microgels/nanogels [4,71,76,120–122]. However, in order to avoid microscopic gelation, the concentration of monomers in water (reaction media) should be kept low. In addition, this method also needs the purification of the resulting polymers by removal of residual monomers and initiators from reaction mixtures.

1.2. Activators generated by electron transfer for ATRP (AGET ATRP)

ATRP is one of the most successful CRP techniques, enabling the preparation of a wide spectrum of polymers with predetermined molecular weight and relatively narrow molecular weight distribution ($M_w/M_n < 1.5$) [56,59,73,123–126]. ATRP also allows for the preparation of copolymers with different chain architectures, such as block, random, gradient, comb-shaped, brush, and multi-armed star copolymers [57,58,77,127–134]. In addition, ATRP has been utilized to prepare polymer–protein/peptide bioconjugates [135–142], polymer-modified polysaccharides [143–148], micellar nanoparticulates [149–155], hydrogels and nanogels [80], ligands stabilizing metal nanocrystals for cellular imaging [156–159], surface-initiated brushes [70,160–163], and emulsion particles [164–166].

The mechanism of ATRP is based on a rapid dynamic equilibration between a minute amount of growing radicals and a large majority of dormant species [59,123,167–170]. In a normal ATRP process (Fig. 3), transition metal complexes in a lower oxidation state ($Cu(I)/L_m$) are added directly to the reaction as an activator, which reacts reversibly with the dormant species (RX) to generate a deactivator ($X–Cu(II)/L_m$) and an active radical (R•). The radical can propagate by addition of monomers (M), and is rapidly deactivated by reaction with $X–Cu(II)/L_m$, regenerating $Cu(I)/L_m$ and a halogen-terminated polymeric chain. Activators generated by electron transfer, (AGET) ATRP is a recently developed initiating process for ATRP with the benefit of addition of a more stable catalyst complex to the reaction mixture. This process uses reducing agents, such as tin(II) 2-ethylhexanoate in organic solvents or ascorbic acid in aqueous solutions, which react with $Cu(II)/L_m$ catalyst precursors to generate the active $Cu(I)/L_m$ catalysts. The process then follows normal ATRP. This AGET ATRP method has been successfully conducted in various homogeneous media including

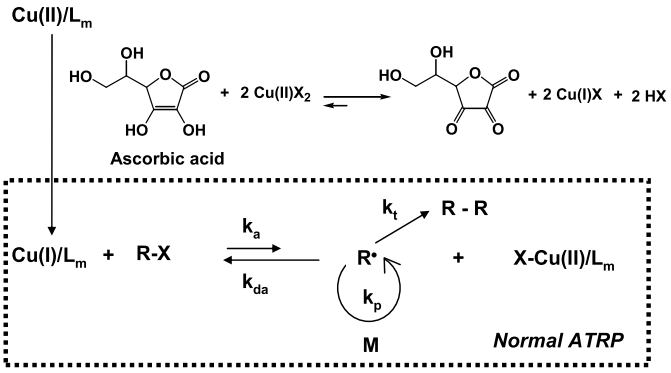

Fig. 3. Mechanism of AGET ATRP, where k_a, k_{da}, k_p, and k_t are the rate constants of activation, deactivation, propagation, and termination, respectively.

bulk [171–174], protic [175], and aqueous solution [176] as well as heterogeneous media including microemulsion [177], *ab initio* emulsion [178], miniemulsion [179–183], dispersion [184], and inverse miniemulsion [79,81].

2. Preparation of non-crosslinked particles by AGET ATRP in inverse miniemulsion

2.1. Particles of well-controlled water-soluble POEOMA

OEOMA is a water-soluble methacrylate-based macromonomer with pendent oligo(ethylene oxide) (OEO) chain. Several grades of OEOMA, with different OEO chain lengths are commercially available, including OEOMA300 ($M = 300$ g/mol, pendent EO units ≈ 5), OEOMA475 ($M = 475$ g/mol, pendent EO units ≈ 9), and OEOMA1100 ($M = 1100$ g/mol, pendent EO units ≈ 23), as shown in Fig. 4. OEOMA is an analogue of linear poly(ethylene oxide) (PEO), which is biocompatible and prevent nanoparticle uptake by reticularendothelial system (RES) [185].

Many requirements should be met in order to conduct a successful ATRP in inverse miniemulsion. One of the requirements is colloidal stability. This mainly involves the selection of the correct surfactants to form stable aqueous monomer droplets, and the resulting polymeric particles, in a continuous oil phase such as cyclohexane. Span 80 (sorbitan monooleate) formed stable inverse miniemulsions of OEOMA with water in cyclohexane, resulting in the formation stable POEOMA particles. The use of water as a solvent was necessary to stabilize aqueous phase as well as a lipophobe to build up an osmotic pressure in inverse miniemulsion droplets. Optionally, an addition of high molecular weight poly(ethylene glycol) (PEG) can be added as costabilizer to enhance colloidal stability of POEOMA particles in inverse miniemulsion polymerization.

Other requirements involve selecting suitable conditions for conducting AGET ATRP in water, since the polymerization occurs in the aqueous monomer droplets dispersed in an organic media. All ATRP ingredients including initiator, catalyst, ligand, and reducing agent should be soluble in water. Various water-soluble, high molecular weight PEO-functionalized bromoisobutyrate initiators were synthesized [176], producing PEO-b-POEOMA block copolymers. They include monofunctional PEO_{113}-Br, PEO_{45}-Br, and bifunctional Br-PEO_{77}-Br (the numbers in subscript indicate the degree of polymerization of the EO units). Dissociation of Br–Cu(II) bond, present in the ATRP deactivator, in water could result in a reduction of the rate of deactivation, leading to a loss of control [186]. Since tri[(2-pyridyl)methyl]amine (TPMA) is known to provide an active water-soluble complex with a low tendency for disproportionation [187], the use of TPMA [186] as the ligand forming the $CuBr_2$ catalyst precursor complex overcomes such

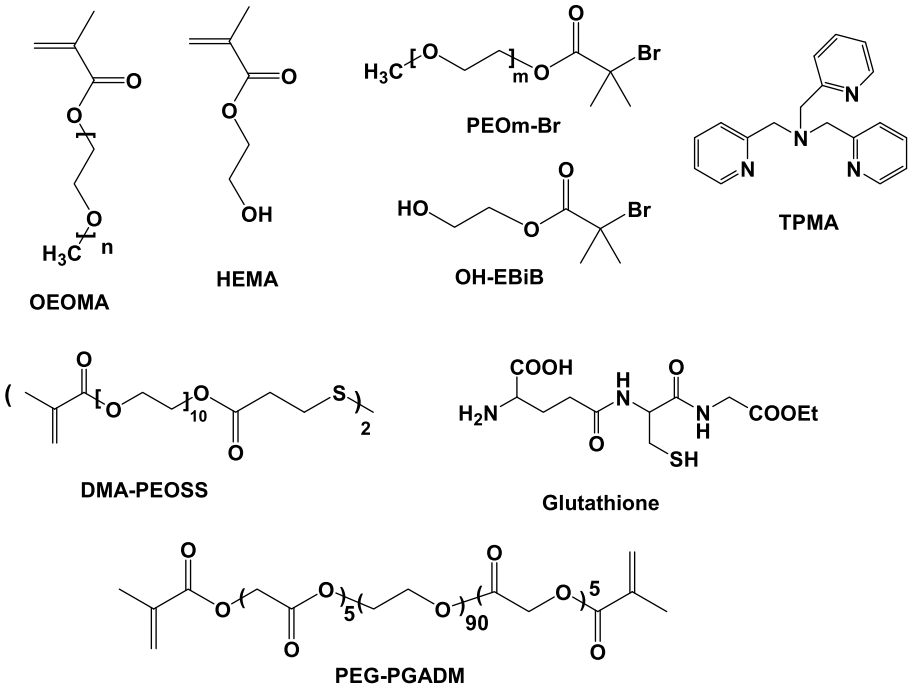

Fig. 4. Chemical structures of reagents used for AGET ATRP inverse miniemulsion.

problems. Water-soluble ascorbic acid (AscA) was typically used as the reducing agent.

Table 1 summarizes the AGET ATRP of OEOMA in cyclohexane inverse miniemulsion conducted with various OEOMA monomers and PEO-based macroinitiators (entries 1–4), targeting DP = 600 (entry 5), and block copolymerization (entry 6). All polymerization produced well-controlled PEO-b-POEOMA and PEO-b-POEOMA300-b-PEOMA475 copolymers with narrow molecular weight distributions ($M_w/M_n < 1.3$). In addition, all polymerization produced nanometer-sized particles with narrow and monomodal size distribution.

2.2. Hydroxy-functionalized particles of well-controlled water-soluble POEOMA

Water-soluble 2-hydroxyethyl 2-bromoisobutyrate (OH-EBiB) has been utilized for the synthesis of hydroxy-functionalized polymers [58] and hydroxy-telechelic polymers [188–191]. OH-EBiB was used as a water-soluble ATRP initiator for AGET ATRP of OEOMA targeting DP = 300 in cyclohexane inverse miniemulsion [102], creating submicron-sized particles of well-controlled OH-functionalized POEOMA at the end of chains (entries 7 and 8, Table 1). In both reactions, conversions reached 75–80%, producing well-controlled polymers with $M_w/M_n < 1.3$. The purified OH-POEOMA was further functionalized with biotin, RGD tripeptide, and pyrene (a fluorescent dye) demonstrating the facile functionalization of crosslinked nanogels with cell-targeting agents for targeted drug delivery applications [195].

2.3. Particles of well-controlled water-swellable PHEMA

Hydroxyethyl methacrylate (HEMA) is a water-soluble monomer, but PHEMA is water-swellable polymer. A stable miniemulsion of HEMA was formed when poly(ethylene-co-butylene)-block-poly(ethylene oxide) (PO-b-PEO) (M_n = 8100 g/mol and 41 wt% of EO) was used as a surfactant for a stable inverse miniemulsion of HEMA and PHEMA. An AGET ATRP of HEMA targeting DP = 300 in an inverse miniemulsion yielded well-controlled PEO-b-PHEMA with monomodal GPC curve and low $M_w/M_n < 1.3$ at 78% monomer conversion (entry 9, Table 1). A well-controlled $PHEMA_{80}$-b-PEO_{77}-b-$PHEMA_{80}$ triblock copolymer was also prepared in the presence

Table 1
Detailed experimental conditions, conversion, and molecular weight data of PEO-b-POEOMA and PEO-b-PHEMA prepared by AGET ATRP in inverse miniemulsion at 30 °C.[a]

Entry	Monomer[b]	Initiator (I)	$[M]_0/[I]_0/[CuBr_2/TPMA]_0$	$[AscA]_0$[c] (mol%)	Conv (%)	$M_{n,th}$[d] (g/mol)	$M_{n,exp}$[e] (g/mol)	M_w/M_n[e]	Diameter (nm)
1	OEOMA300	PEO_{113}-Br	300/1/0.5	90	73	71,200	71,100	1.29	120–150
2	OEOMA300	PEO_{45}-Br	300/1/0.5	90	73	68,200	64,100	1.23	174
3	OEOMA475	PEO_{45}-Br	300/1/0.5	70	88	119,500	127,500	1.35	212
4	OEOMA1100	PEO_{113}-Br	70/1/0.5	70	88	73,000	67,200	1.29	185–210
5	OEOMA475	PEO_{113}-Br	600/1/1	70	62	182,000	81,000	1.32	143
6	OEOMA475	POEOMA300-Br	223/1/0.6	90	85	64,100	68,500	1.30	226
7	OEOMA475	OH-EBiB	300/1/0.5	70	80	114,000	72,000	1.25	
8	OEOMA300	OH-EBiB	300/1/0.5	150	75	67,500	25,000	1.3	
9	HEMA	PEO_{113}-Br	300/1/0.5	70	78	35,400	49,400	1.29	

[a] Conditions for inverse miniemulsion AGET ATRP: monomer/water = 1/1 v/v; solids content = 10 wt%.
[b] Surfactant: Span 80 for OEOMA and PO-b-PEO for HEMA.
[c] Based on $[CuBr_2/TPMA]_0$.
[d] $M_{n,th}$ = MW (I) + MW(monomer) × ($[monomer]_0/[I]_0$) × conversion.
[e] Calibrated with PMMA standards.

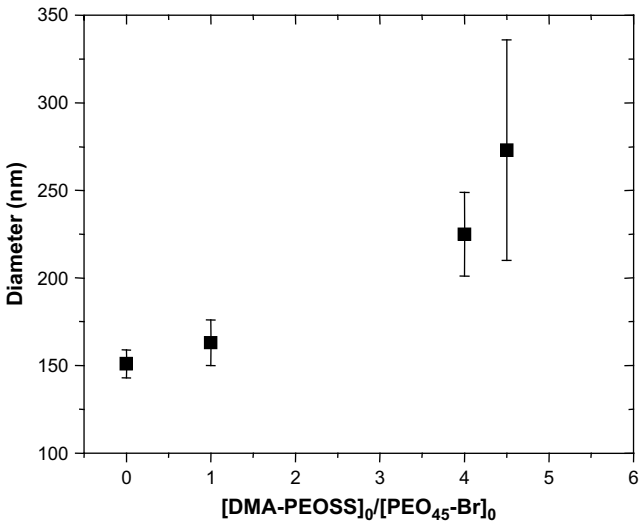

Fig. 5. An increase of size of POEOMA300 nanogels prepared by AGET ATRP of OEOMA300 in cyclohexane inverse miniemulsion in the presence of different amounts of DMA-PEOSS. Conditions: $[OEOMA300]_0/[PEO_{45}\text{-}Br]_0/[CuBr_2/TPMA]_0/[AscA]_0 = 300/1/0.5/0.35$; OEOMA300/water = 1/1 v/v; solids content = 10 wt%. The diameter of nanogels dispersed in cyclohexane was measured by DLS.

of difunctional Br-PEO_{77}-Br macroinitiator. PHEMA, with DP = 80, is not soluble in water while PEO is soluble in water. Consequently, the resulting block copolymers self-assembled to form micellar nanoparticles consisting of 9 – 10 $PHEMA_{80}$-b-PEO_{77}-b-$PHEMA_{80}$ triblock copolymers with a diameter = 13 nm in water [81].

3. Preparation of nanogels crosslinked with biodegradable linkages by inverse miniemulsion ATRP

3.1. Nanogels crosslinked with degradable disulfide linkages

The synthesis of dithiopropionyl poly(ethylene glycol) dimethacrylate (DMA-PEOSS, Fig. 4), a water-soluble disulfide-functionalized crosslinker, was reported elsewhere [78]. A series of biodegradable crosslinked nanogels of well-controlled POEOMA300 were prepared by AGET ATRP of OEOMA300 targeting DP = 300 in inverse miniemulsion in the presence of different amounts of DMA-PEOSS. As shown in Fig. 5, the sizes of crosslinked particles were larger than those of uncrosslinked particles dispersed in cyclohexane. As the ratio of $[DMA\text{-}PEOSS]_0/[PEO_{45}\text{-}Br]_0$ increased, the size and size distribution of nanogels increased. For the ratio of $[DMA\text{-}PEOSS]_0/[PEO_{45}\text{-}Br]_0 > 4/1$, the resulting particles did not dissolve in solvents, including THF and water.

Fig. 6 shows AFM height and phase images of uncrosslinked and crosslinked POEOMA300 particles on mica surfaces. The particle

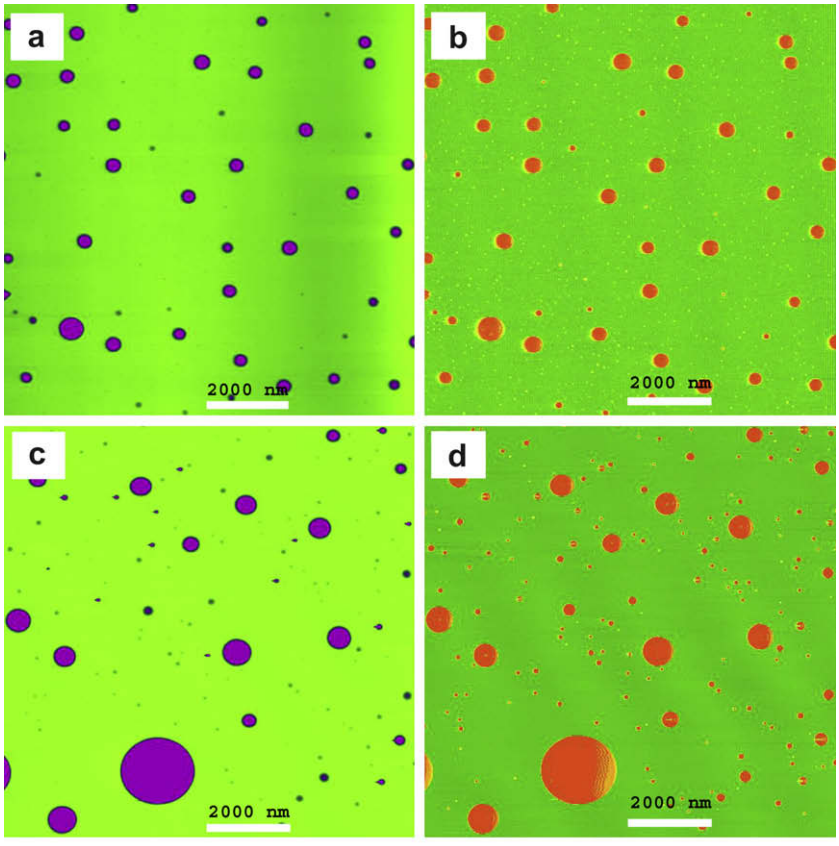

	$H_{n,av}$ (nm)	$H_{w,av}/H_{n,av}$	$D_{n,av}$ (nm)	$D_{av,w}/D_{av,n}$
Uncrosslinked	18 ± 6	1.11	310 ± 88	1.08
Crosslinked	55 ± 23	1.17	425 ± 171	1.15

Fig. 6. AFM height (a and c) and phase (b and d) images of uncrosslinked (a and b) and crosslinked (c and d) POEOMA300 particles prepared with $[DMA\text{-}PEOSS]_0/[PEO_{45}\text{-}Br]_0 = 4/1$ by inverse miniemulsion ATRP at 30 °C. Each image frame is 10 μm × 10 μm. Reprinted with permission from Ref. [78]. Copyright 2006 American Chemical Society.

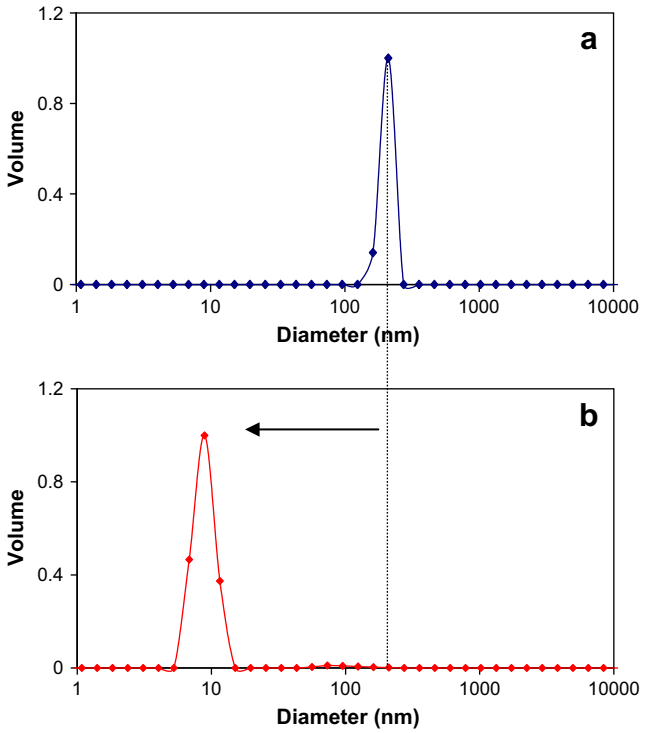

Fig. 7. CONTIN plots for RITC-Dex loaded POEOMA300-co-PHEMA nanogels before (a. Size: 203 nm, CV = 0.48) and after acid catalyzed hydrolysis (b. Size: 9 nm, CV = 0.44).

size distribution for uncrosslinked particles was uniform. Their average diameter determined by AFM analysis was 310 nm, i.e. ~2 times larger than that determined by DLS (145 nm). The difference is due to flattening of the particles on the mica surface during the casting process, as confirmed by their small height (18 nm). For crosslinked particles prepared with $[DMA\text{-}PEOSS]_0/[PEO_{45}\text{-}Br]_0 = 4/1$, the particle size distribution was broader. However, the difference of particle diameter determined by AFM and DLS decreased; the ratio of the sizes determined by AFM (425 nm) to that by DLS (260 nm) was 1.6 times. This is because crosslinked particles spread out on the mica surface to a lesser degree, as confirmed by their relatively greater height (55 nm compared to 18 nm) [78].

3.2. Nanogels crosslinked with hydrolyzable polyester linkages

Recently, poly(ethylene glycol)-co-poly(glycolic acid) dimethacrylate (PEG-PGADM) was synthesized [192–194] and used as an hydrolyzable crosslinker for the preparation of biodegradable POEOMA300-co-PHEMA nanogels by AGET ATRP. These nanogels degraded upon hydrolysis of oligo(α-hydroxy acid)s into water-soluble polymers, as decreasing the diameter from 203 nm to 9 nm (Fig. 7). The degraded polymers residues with low molecular weights can be facilitated for excretion from the body via renal filtration in an *in vivo* application.

3.3. OH-functionalized biodegradable nanogels

The preparation of functionalized nanogels is required to allow bioconjugation of the nanogels for targeted drug delivery applications. Two approaches were examined for the preparation of OH-functionalized nanogels crosslinked with disulfide and polyester linkages (Fig. 8). One approach involves an introduction of functional monomers, particularly 2-hydroxyethyl acrylate (HEA, 10 mol% of OEOMA) at certain conversion (ca. 30%) during inverse miniemulsion ATRP of OEOMA300 in the presence of DMA-PEOSS. This approach enabled preparation of functional nanogels of PEO-b-POEOMA-b-P(OEOMA-co-HEA) block copolymers with pendent OH groups. The average particle size was 225 ± 24 nm for the homopolymeric nanogels and 236 ± 29 nm for OH-containing nanogels, indicating an average increase in the size of the OH-nanogels by 10 nm after the addition of HEA [80]. Similarly, HEMA (25 mol% of OEOMA) was copolymerized with OEOMA300 in the presence of PEG-PGADM crosslinker, producing hydrolyzable OH-functionalized nanogels. The resulting POEOMA300-co-PHEMA nanogels with a diameter of 203 ± 11 nm were stable in water over a long period of time (7 days) without any sign of precipitation. Another approach involves the use of an OH-EBiB initiator for AGET ATRP of OEOMA300 in cyclohexane inverse miniemulsion in the presence of DMA-PEOSS. Functional nanogels of PEO-b-PEOMA300 with terminal OH groups were prepared [102].

4. Comparison of nanogels prepared by ATRP with those by conventional FRP

A conventional free-radical polymerization (FRP) of OEOMA300 in inverse miniemulsion in cyclohexane in the presence of 1.5 mol% DMA-PEOSS was initiated with 2,2-azobis(4-methoxy-2,4-dimethyl valeronitrile) (V-70, Wako Chemie) at 40 °C, resulting in the formation of FRP-nanogels. Fig. 9 compares the swelling ratios of ATRP-nanogels with these FRP-nanogels in different solvents including THF, toluene, and water. The swelling ratios of the nanogels were determined by the weight ratio of wet gels to dried gels. For ATRP gels, the swelling ratios ranged from ~20 in organic solvents (THF and toluene) to ~28 in water. These values were 1.6–1.8 times larger than those for FRP gels in all solvents examined. This difference could be ascribed to crosslinks being more evenly distributed in ATRP-nanogels. Furthermore, FRP-nanogels were not degraded in the presence of tributyl phosphine (Bu_3P) in THF (see

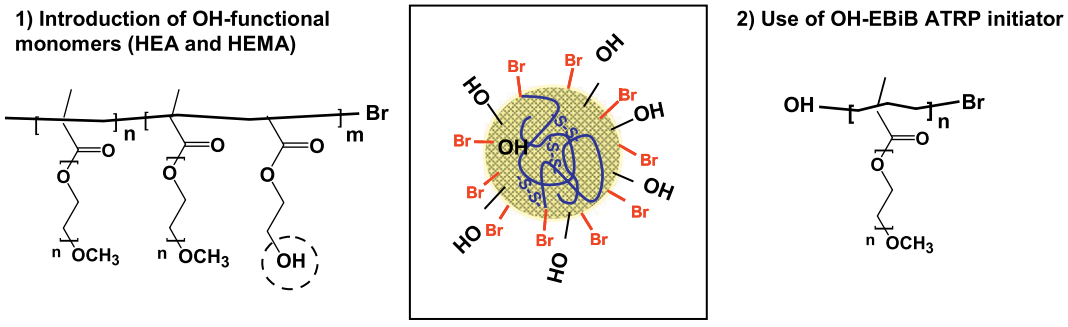

Fig. 8. Two approaches to prepare OH-functionalized biodegradable nanogels by ATRP of OEOMA in inverse miniemulsion.

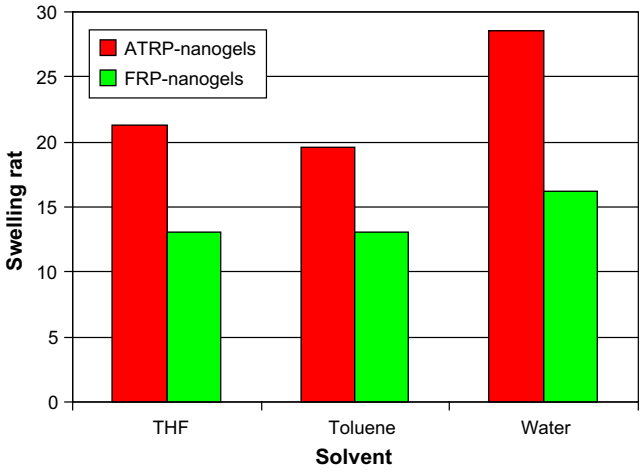

Fig. 9. Comparison of swelling ratio of degradable nanogels prepared by inverse miniemulsion using ATRP and FRP in various solvents. Both gels were prepared in the presence of 1.5 mol% DMA-PEOSS. Swelling ratios of nanogels were determined by the weight ratio of wet gels to dried gels.

Section 7 for details). These results clearly demonstrated that inverse miniemulsion ATRP in the presence of a crosslinker resulted in the formation of nanogels with a uniform network structure. The ATRP-nanogels had larger swelling ratios than FRP-nanogels in various solvents. They could be redispersed in water to form stable hydrogels with a large swelling ratio of 28.

5. Live/dead cytotoxicity of nanogels and degraded polymers

The cytotoxicity of nanogels and their degradation products in the presence of glutathione was examined using the LIVE/DEAD Viability/Cytotoxicity. An aliquot of nanogels and degraded nanogels was cultured with HeLa cells. After 24 h incubation, fluorescence microscopy was used to visualize live (green fluorescence) and dead (red fluorescence) cells. Fig. 10 shows the combined images for live and dead HeLa cells in the presence of nanogels. The viability of HeLa cells was 89% in the presence of nanogels an 94% in the presence of degraded nanogels, compared with 95–96% in the their absence as a control experiment. These results suggest that POEOMA nanogels prepared by inverse ATRP miniemulsion, and the degraded nanogels in the presence of glutathione, are non-toxic to cells and biocompatible [80].

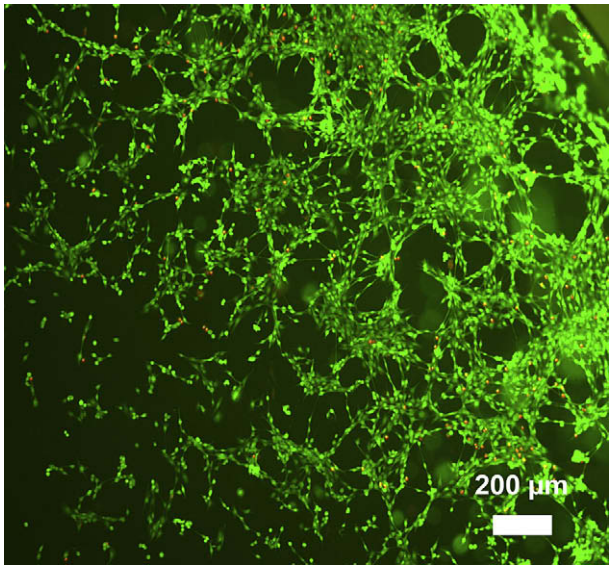

Fig. 10. Fluorescent image of live (green) and dead (red) HeLa cells after 24 h incubation with nanogels. The gels were purified by extensive dialysis in water for 7 days. Scale bar = 200 μm. Reprinted with permission from Ref. [80]. Copyright 2007 American Chemical Society.

6. Loading of fluorescent dyes, biomolecules, polymers, and inorganic nanoparticles into nanogels

Several methods were utilized to incorporate various water-soluble and dispersible (bio)molecules into the nanogels. They include incorporation of fluorescent dyes, anticancer drugs, gold nanoparticles (AuNPs), high molecular weight carbohydrate and protein drugs, and star branched polymers. Low molecular weight fluorescent dyes, anticancer drugs, and AuNPs were physically loaded into purified nanogels (physical loading), while high molecular weight biomolecules such as carbohydrates and proteins were physically incorporated into nanogels during the inverse miniemulsion ATRP (*in-situ* physical incorporation). Star branched polymeric nanoparticles having ATRP bromine initiating moieties were covalently incorporated into nanogel networks during inverse miniemulsion ATRP (*in-situ* covalent incorporation).

6.1. Physical loading of Rhodamine 6G, Doxorubicin, and AuNPs

Nanogels prepared by inverse miniemulsion ATRP in cyclohexane were first purified by precipitation in THF, followed by centrifugation to remove THF-soluble species, including unreacted OEOMA300 and Span 80 (surfactant). The dried nanogels were fully swollen in water and then magnetically stirred with various amounts of Rhodamine 6G (R6G, expressed as the wt ratio of R6G to nanogel in water) for 3 days at room temperature. After the mixtures were transferred into a dialysis tubes (MWCO = 6–8 kDa) in water, an aliquot of outer water was periodically taken for UV–vis measurements. Using the pre-constructed calibration curve of R6G and its extinction coefficient ($\varepsilon = 80{,}000\ M^{-1}\,cm^{-1}$ at $\lambda = 526$ nm) in water, the amount of free R6G dyes removed from the mixture through dialysis tubing was determined.

Fig. 11a shows the wt% of accumulated R6G in outer water to originally added R6G. In a controlled experiment conducted only with R6G, without nanogels, the wt% reached 100% within 3 days, indicating complete removal of all R6G dyes from the dialysis tube. In all experiments with different weight ratios of R6G/nanogel, a plateau of wt% was observed after 3 days. Consequently, the loading level of R6G in the nanogels (i.e. amount of R6G remaining in the nanogels) was calculated after 3 days. As seen in Fig. 11b, the loading level increased with the wt ratio of R6G/nanogel and reached a plateau at 34% with wt ratio of R6G/nanogel > 1.5.

Doxorubicin (Dox, called adriamycin or hydroxyldaunorubicin) is an amphiphilic DNA-interacting drug widely used in chemotherapy and has been physically entrapped in hydrogels [96,120]. In the experiments [96], Dox was also loaded into nanogels in water, using a similar procedure to that used for R6D loading. The loading level was determined using the extinction coefficient of Dox ($\varepsilon = 7600\ M^{-1}\,cm^{-1}$ at $\lambda = 497$ nm) in water. The loading level of Dox into nanogel increased from 5.4 to 16.4 wt% as the initial ratio of Dox/nanogel in mixture increased from 0.07/1 to 0.35/1. Such increase is due to an increase in extent of both hydrophobic and hydrophilic interactions between Dox and OEO segments, because they have amphiphilic character. Similar results were observed for nanogels based on Pluronic F127 containing hydrophobic poly(propylene glycol) where the amount of Dox loaded into nanogels increased from 2.7 to 8.9 wt% as the initial ratio of Dox/nanogel increased from 0.1/1 to 0.2/1 [96].

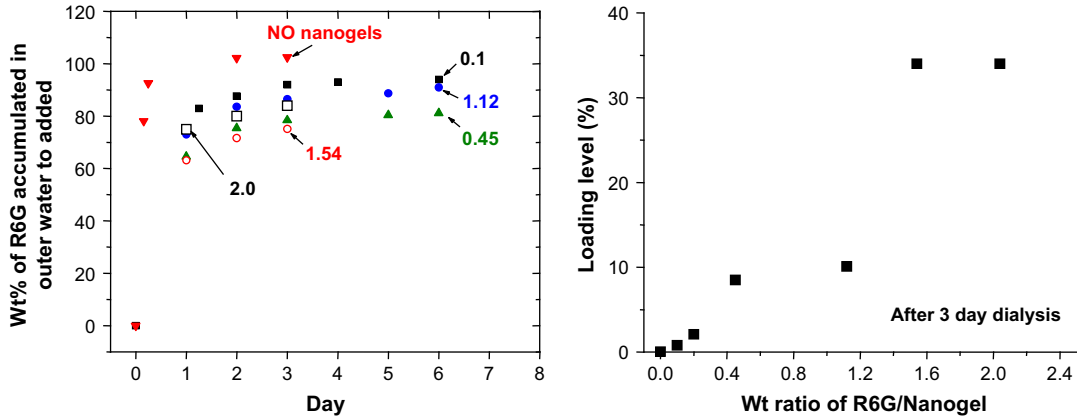

Fig. 11. Wt% of accumulated R6G in outer water to originally added R6G with days for extensive dialysis (a) and loading level of R6G vs. wt ratio of R6G/nanogel determined after 3 day dialysis (b). The amount of R6G was determined using UV–vis spectroscopy with Beer–Lambert equation and extinction coefficient of R6G (80,000 M^{-1} cm^{-1}) in water. The figures in the plot (a) indicate wt ratio of R6G/nanogel.

Inorganic gold nanoparticles (AuNPs) with a diameter of 2 nm were incorporated by mixing POEOMA300 nanogels (2.45 mg/mL) with AuNPs (0.25 mM) in water for 2 days. Unabsorbed AuNPs were removed by dialysis tubing (MWCO = 12–14 kDa) in water. Thermogravimetric analysis suggested that each AuNP-loaded nanogel contained approximately 3000 AuNPs, corresponding to 42% by mass or 3.6% by volume [195]. The results are promising for site-specific drug delivery and photodynamic therapy (PDT) applications [196].

6.2. In-situ physical incorporation of high molecular weight carbohydrates and proteins

High molecular weight biomolecules such as carbohydrates, proteins, and DNA as model water-soluble macromolecular drugs were incorporated into microgels during heterogeneous free-radical polymerization. A few reports described the preparation of dextran (Dex)-loaded hydrogels by post-polymerization crosslinking of poly(*N*-isopropylacrylamide-co-allylamine) microgels with glutaric dialdehyde in the presence of Texas Red-labeled dextran [197], crosslinked poly(vinyl pyrrolidone) nanoparticles in the presence of fluorescein isothiocyanate-labeled dextran using a reverse micellar technique [115,116], and polyacrylamide microgels in the presence of ovalbumin and plasmid DNA by inverse miniemulsion polymerization [99,100].

Biodegradable POEOMA nanogels loaded with rhodamine isothiocyanate-labeled dextran (RITC-Dex) were prepared by inverse miniemulsion ATRP in the presence of 1.5 mol% DMA-PEOSS. Different amounts of water-soluble RITC-Dex (2.9, 6.8, and 8.2 wt%) were introduced into the aqueous solution stably dispersed in an organic continuous phase, resulting in the formation of pink-colored dispersions of crosslinked RITC-Dex-containing POEOMA nanogels. The particle size of nanogels prepared in the presence of up to 6.8 wt% RITC-Dex was ca. 245–250 nm in diameter. The resulting RITC-Dex-loaded nanogels biodegraded in the presence of reducing agents (the detailed reductive degradation will be described in the following section). This degradability allowed use of UV–vis spectroscopy to determine the degree of incorporation of RITC-Dex into the nanogels. A linear calibration curve of the absorbance at 555 nm vs. amount of RITC-Dex was constructed from UV–vis spectra of various amounts of RITC-Dex in water. A known amount of the purified dried RITC-Dex-containing nanogels was mixed with glutathione (15 wt% of nanogels) in water at room temperature for 1 day, resulting in the formation of a transparent pink solution upon degradation of the nanogel. The UV–vis spectra of the solutions were measured. The amount of RITC-Dex loaded in nanogels was calculated from the absorbance at the wavelength and the calibration curve (Table 2). The extent and efficiency of incorporation of RITC-Dex in nanogels prepared in the presence of 2.9 wt% RITC-Dex, was 2.4 wt% and 84 wt%, respectively. When the amount of RITC-Dex was increased from 2.9 to 6.8 wt%, the extent of incorporation was 5.5 wt%, resulting in slight decrease in efficiency to 81% [82].

Nanogels prepared with HO-EBiB as an ATRP initiator were utilized to load bovine serum albumin (BSA) into OH-functionalized nanogels. The resulting nanogels had a diameter of 132 nm with narrow size distribution by DLS (Fig. 12a). A slightly smaller size was observed by transmission electron microcopy (TEM) (Fig. 12b). The resulting crosslinked BSA-containing OH-POEOMA nanogels were biodegraded into the corresponding thiol-containing polymers, releasing BSA in a controlled manner.

6.3. In-situ covalent incorporation of bromine-functionalized star branched nanoparticles

Well-defined biodegradable star branched polymeric nanoparticles were prepared by ATRP of a disulfide-functionalized dimethacrylate in the presence of PEO_{113}-Br as a macroinitiator in MeOH. They consist of a hydrophobic biodegradable crosslinked core and ~20 hydrophilic PEO arms with M_n = 10,000 g/mol. The average diameter of the star copolymers measured by DLS was 20–30 nm in MeOH. Fig. 13b shows the GPC traces of star branched polymer before and after degradation. The GPC traces of the star polymer consist of two peaks; a sharp peak for unreacted PEO_{113}-Br

Table 2
Extent of incorporation of RITC-Dex in nanogels prepared by AGET ATRP of OEOMA300 in cyclohexane inverse miniemulsion in the presence of DMA-PEOSS and RITC-Dex at 30 °C.[c]

RITC-Dex added to polymerization (wt%)	Incorporation	
	Level[a] (%)	Efficiency[b] (%)
2.9	4.0	84
6.8	9.1	81

[a] Weight ratio of RITC-Dex to nanogels.
[b] Weight ratio of RITC-Dex incorporated into nanogels to that added to polymerization. Efficiency (%) = level/(amount of RITC-Dex added to polymerization/conversion). The amount of RITC-Dex added to the polymerization was calculated based on monomer conversion to be 60% determined by GPC measurements.
[c] Reprinted with permission from Ref. [82]. Copyright 2007 American Chemical Society.

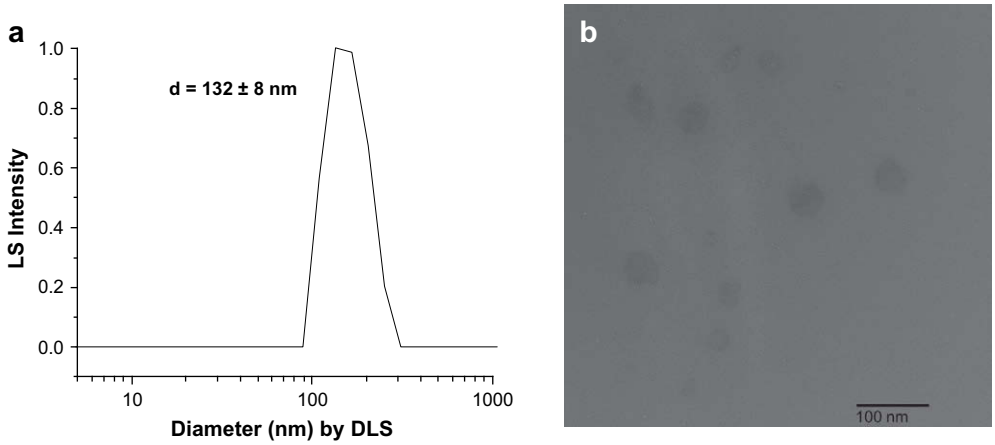

Fig. 12. A CONTIN plot (a) and TEM image (b) of BSA-loaded POEOMA nanogels prepared by AGET ATRP in inverse miniemulsion at 30 °C. Conditions: $[OEOMA300]_0/[HO\text{-}EBIB]_0/[DMA\text{-}PEOSS]_0/[CuBr_2/TPMA]_0/[AscA]_0 = 150/1/4//0.5/0.5/0.55$, OEOMA300/water = 1/1.2 v/v, BSA = 25 wt% of OEOMA300. The scale bar = 100 nm in (b). Reprinted with permission form Ref. [195]. Copyright 2009 American Chemical Society.

with $M_n \approx 10{,}000$ g/mol and a broader peak for high molecular weight star polymers. These polymers degraded into the corresponding thiol-containing polymers in the presence of tri(*n*-butyl)phosphine (Bu_3P) in THF. Since star branched polymers preserve bromine functionality on the surface of particles, they were used as macroinitiators for further ATRP polymerization to prepare mikto-arm star polymers (or star-grafted polymers) [202].

The preparation of mikto-arm star polymers was carried out in cyclohexane inverse miniemulsion using AGET ATRP of OEOMA300 targeting DP = 300. Different amounts of bromine-functionalized star branched polymers (8.6 and 13.4% of OEOMA300) were added to the reactions and all polymerizations produced stable nanometer-sized particles of POEOMA300 covalently embedded with star polymers. The particle diameter measured by DLS was 157 nm for nanogels prepared in the presence of 8.7% star polymer and 230 nm with 13.4% star polymer. Fig. 13a shows that first-order kinetic plots for the polymerizations were linear and that the rate of polymerization was faster in the presence of 13.4% of the star branched polymers than with 8.6%. The GPC trace of the star-grafted POEOMA300 before degradation consisted of two peaks; a smaller sharp peak with $M_n \approx 10{,}000$ g/mol and a broader peak for high molecular weight polymers (Fig. 13b). The height of the former was smaller than that of star branched polymer, while the latter shifted to high molecular weight. This suggests that the resulting nanogels consisted of two types of polymers; PEO_{113}-b-POEOMA300 initiated from unreacted PEO_{113}-Br and POEOMA300 grafted with star branched polymer (star-grafted POEOMA300) initiated from star branched polymer. The resulting star-grafted POEOMA300 degraded into corresponding thiol-containing POEOMA300 in the presence of Bu_3P in THF.

A biodegradable POEOMA300 nanogel covalently embedded with biodegradable star branched polymeric nanoparticles was prepared by AGET ATRP in inverse miniemulsion in the presence of 1.35% DMA-PEOSS and 13.4% star branched polymers. The average number of star nanoparticles embedded in a POEOMA300 particle was estimated to be 55, assuming that the density of star polymer and POEOMA = 1 and the diameter = 30 nm for star nanoparticles. The loading efficiency of hydrophobic drugs into the hydrophobic nanodomain-containing POEOMA nanogels was examined; Pyrene methanol (Py) was selected as a model hydrophobic drug (48 mg) and was mixed with the dried nanogels (0.153 g) in THF for 2 days. The resulting Py-loaded nanogels were isolated and then degraded in the presence of Bu_3P in THF. Using the extinction coefficient of Py ($\varepsilon = 40{,}000\ M^{-1}\,cm^{-1}$ in THF), the loading level of Py into hydrophobic nanodomain-containing nanogels was calculated to be 9.1 wt%, which is twice larger than that (4.9 wt%) for nanogels formed without incorporation of hydrophobic star polymers. These results indicate that the hydrophobic star nanodomains enhanced loading level of hydrophobic or amphiphilic drugs into hydrophilic POEOMA nanogels.

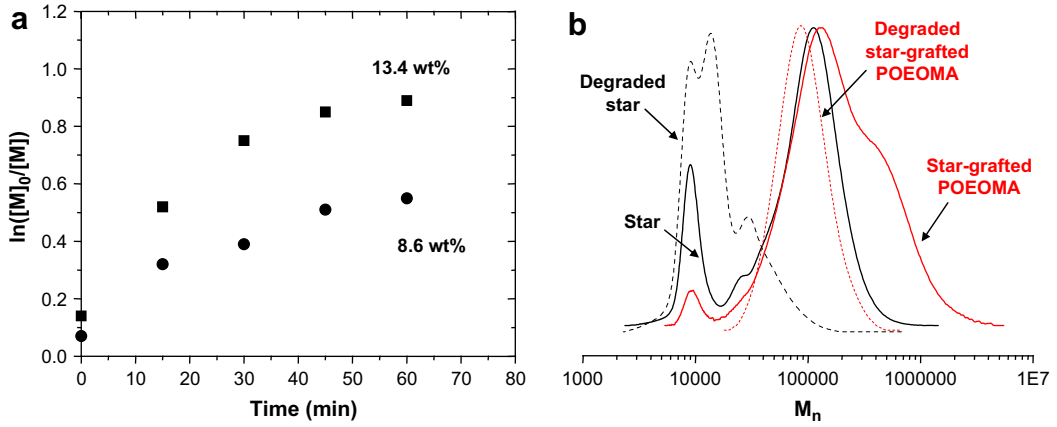

Fig. 13. First-order kinetic plots for AGET ATRP of OEOMA300 targeting DP = 300 in inverse miniemulsion in the presence of different amounts of Br-functionalized star branched polymeric nanoparticles (a) and GPC traces of degradable star branched polymer and star-grafted POEOMA300 before and after degradation in the presence of Bu_3P in THF (b).

7. Degradation of ATRP-nanogels in the presence of reducing agents

Disulfide–thiol chemistry has been widely utilized in conventional polymer syntheses. Disulfides are cleaved to the corresponding thiols under reducing conditions or through disulfide–thiol exchange. Recent reports describe the use of this chemistry to design well-defined degradable polymers [84,198–201], hydrogels [37,202], polymer capsules [203], and micellar particles [204–209]. Therefore, the reductive degradation of crosslinked ATRP-nanogels with disulfide linkages into the corresponding thiol-containing POEOMA300 fragments was investigated with various reducing agents, including Bu_3P, glutathione, and dithioerythritol (DTT) (Fig. 14).

The reductive degradation was initially conducted in the presence of Bu_3P in THF. A known amount of dried nanogels was mixed with a trace amount of Bu_3P in THF and magnetically stirred for 3 days. The degraded polymers were soluble in THF and were characterized using gel permeation chromatography (GPC), $M_n = 74{,}000$ g/mol and $M_w/M_n = 1.5$ [78]. However, since Bu_3P is hydrophobic and toxic to cell, the use of hydrophilic or water-soluble reducing agents to degrade nanogels *in vitro* was examined.

Glutathione is a biocompatible tripeptide found within cells at millimolar concentrations [206,210]. A few reports describe the use of glutathione as a water-soluble reducing agent that can degrade disulfide-containing polymers to the corresponding thiols [205,206]. The extent of degradation of the nanogel was determined by the weight loss of swollen nanogels in the presence of different amounts of glutathione in water over time [80].

Fig. 15 shows the results of degradation. In the absence of glutathione, the weight fraction of nanogels was almost 100%, indicating no significant degradation. However, in the presence of glutathione, the weight fraction of nanogels decreased over time, confirming successful degradation. The degradation rate of nanogels increased with the amount of glutathione. Within 1 h, over 85% nanogels were degraded in the presence of ca. 20 wt% of glutathione (vs. nanogels), while 40% nanogels were degraded in the presence of 10 wt% of glutathione. Thus, nanogels crosslinked with disulfide linkages were successfully degraded in the presence of biocompatible reducing agents such as glutathione into the corresponding thiol-containing polymers.

8. Controlled release of encapsulated molecules from nanogels upon degradation

This section describes controllable release of encapsulated molecules, including fluorescent dyes and anticancer drugs, upon degradation of nanogels in the presence of glutathione.

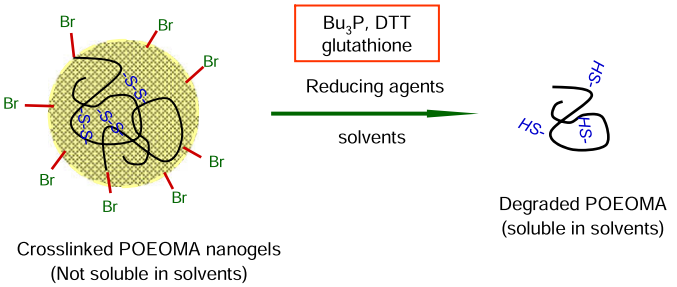

Fig. 14. Schematic representation of reductive degradation of crosslinked ATRP-nanogels into corresponding thiol-containing POEOMA segments in the presence of various reducing agents.

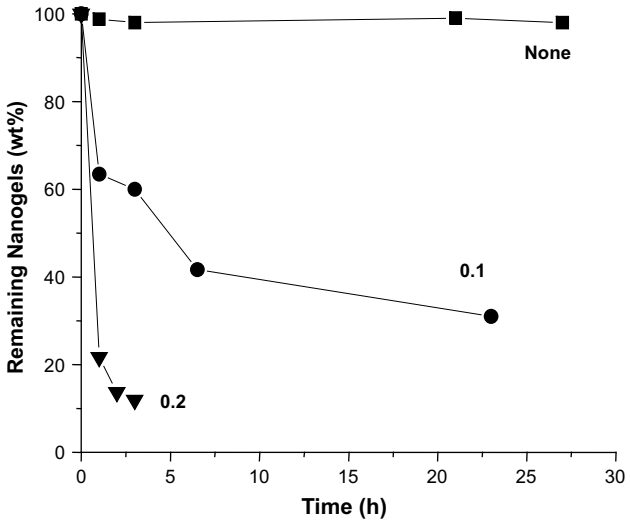

Fig. 15. Evolution of weight fraction of remaining nanogels over time in the presence of different amounts of glutathione, expressed as wt ratio of glutathione/nanogels. Reprinted with permission from Ref. [80]. Copyright 2007 American Chemical Society.

8.1. In vitro release of R6G in cellular media

The preparation of POEOMA nanogels loaded with 34% R6G by the physical loading method was described in the Section 6.1. When compared to the Optical Fluorescence Microscopy (OFM) image of nanogels without fluorescent dyes (Fig. 16a), the distinct bright spots on the dark background indicate that dyes were localized in the nanogel particles (b). In contrast, a diffuse fluorescent signals in the background points out the release of dyes from the nanogels upon addition of glutathione in water (c). These results confirm that degradation of the nanogels could trigger the controllable release of encapsulated drugs in a reducing environment [80].

In vitro release of R6G from R6G-loaded nanogels upon degradation was demonstrated in cellular environments. Before the addition of glutathione to a mixture of C2C12 cells incubated with R6G-loaded nanogels, the red fluorescence was localized in the large R6G-loaded nanogels (Fig. 17a). When glutathione was added, nanogels were degraded releasing the R6G dye, which entered and stained the cells, as shown in Fig. 17b [80].

8.2. In vitro release of Dox to kill HeLa cells

The preparation of POEOMA300 nanogels loaded with 16.4% Dox was described in Section 6.1. HeLa cancer cells were incubated with and without 16.4% Dox-loaded nanogels. After 48 h, the cell viability was measured using live/dead staining to estimate the cytotoxicity of the Dox-loaded nanogel before addition of the reducing agent. After performing this analysis, glutathione was added to the wells containing the nanogels and free Dox was added to some of control wells without nanogels. The resulting mixtures were maintained for another 24 h. As seen in Fig. 18, before addition of glutathione, the viability of HeLa cells in the presence of Dox-loaded nanogels was similar to the control. This suggests that most Dox remained in the nanogels without any significant level of non-specific leaching of Dox from the nanogels. This minimization of non-specific release of drugs during circulation in the blood is important for *in vivo* application of the nanogels as drug delivery carriers. Upon addition of glutathione, the nanogels were degraded and released Dox to kill HeLa cells. From an analysis based on live/dead cytotoxicity assays after Dox release, the cell viability was ca. 52% in the presence of Dox-loaded nanogels, which is lower than that for the control (93%) but

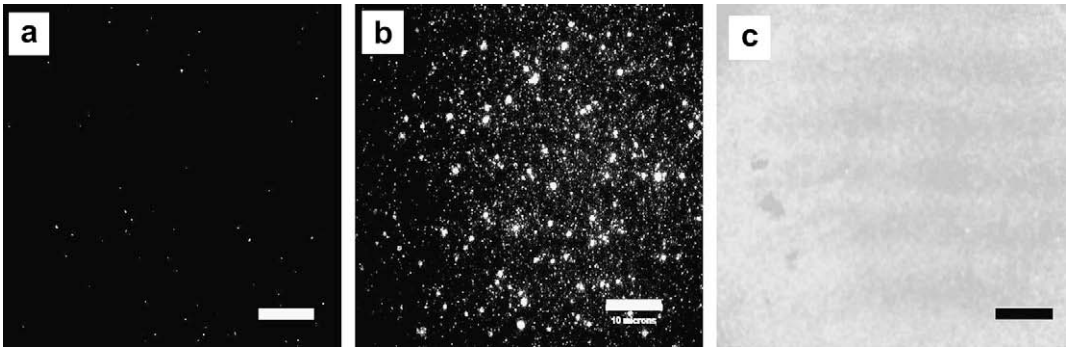

Fig. 16. OFM images of nanogels loaded without (a) and with (b) R6G fluorescent dyes before and (c) after degradation in the presence of glutathione in water. Thin films were spin-cast on a cleaned glass plate and dried at room temperature for 10 min. All scale bars = 10 μm. Reprinted with permission from Ref. [80]. Copyright 2007 American Chemical Society.

around 7 times higher than that in the presence of free Dox (7%). However, the level of viability is similar in both cases, since the amount of free Dox added to the wells was 6–7 times larger than the amount of Dox in the Dox-loaded nanogels. This experiment demonstrated that the Dox-loaded nanogels are essentially non-toxic before addition of the reducing agent (48 h mark in the graph), but after the reducing agent is added, the drug is released, and the cell growth is significantly inhibited due to the presence of released Dox (72 h mark) [80].

8.3. Release of RITC-Dex for specific binding to lectins

The preparation of RITC-Dex-loaded nanogels was described in Section 6.2. RITC-Dex released from nanogels upon degradation in a reducing environment could bind to specific bio-targets such as lectins. ConA is a well known protein that simultaneously binds to glucose (homotetramer) at neutral pH [211–214].

A known amount of RITC-Dex-loaded nanogels was degraded in the presence of glutathione in PBS buffer for 1 day. FT-IR was used to measure the % transmittance (*T*%) at 700 nm of the resulting transparent solution and was determined to be 93%. An aliquot of ConA solution was then added to the transparent solution at weight ratio of ConA/RITC-Dex = 7.0. The transmittance at 700 nm for the solution was monitored as a function of time. The results could be compared with those obtained with free RITC-Dex and ConA under similar conditions (Fig. 19). For both systems, the % transmittance decreased with time and reached a plateau after 2 days. These results suggest the formation of aggregates by interacting RITC-Dex

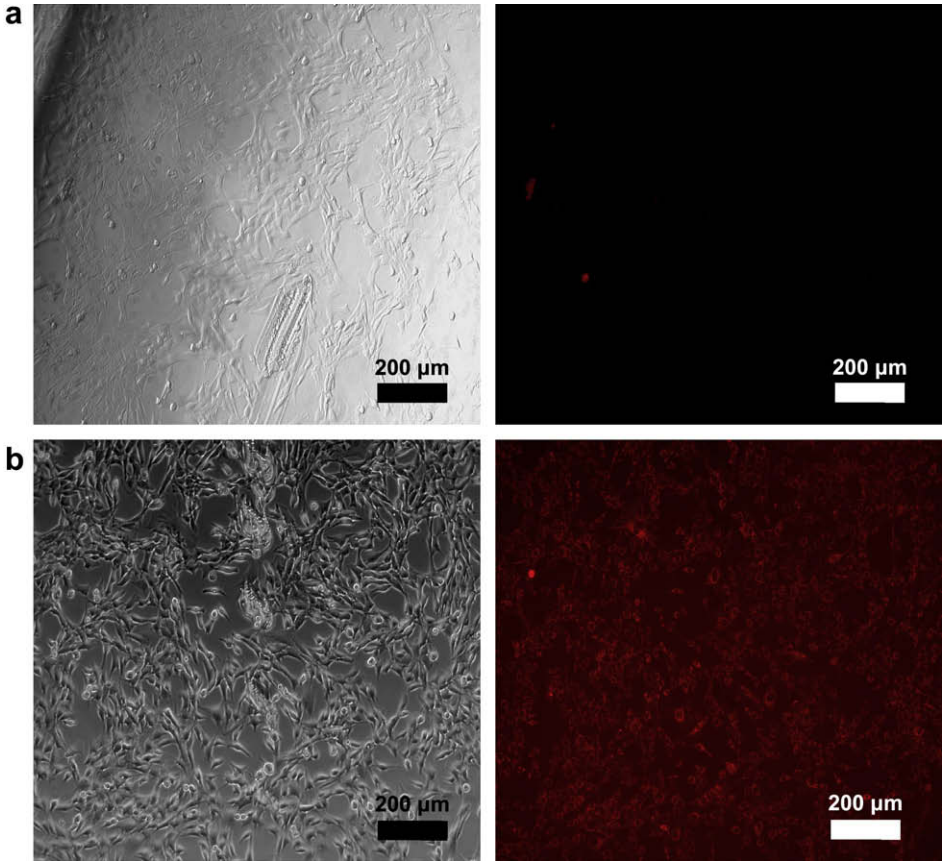

Fig. 17. Differential interference contrast (DIC) (left) and fluorescent (right) images of C2C12 cells, after 24 h incubation with R6G-loaded nanogels (a), and after another 24 h incubation with R6G-loaded nanogels in the presence of glutathione (b). The red fluorescence originates from R6G loaded (right in a) to and released (right in b) from nanogels. All scale bars = 200 μm. All scale bars = 10 μm. Reprinted with permission from Ref. [80]. Copyright 2007 American Chemical Society.

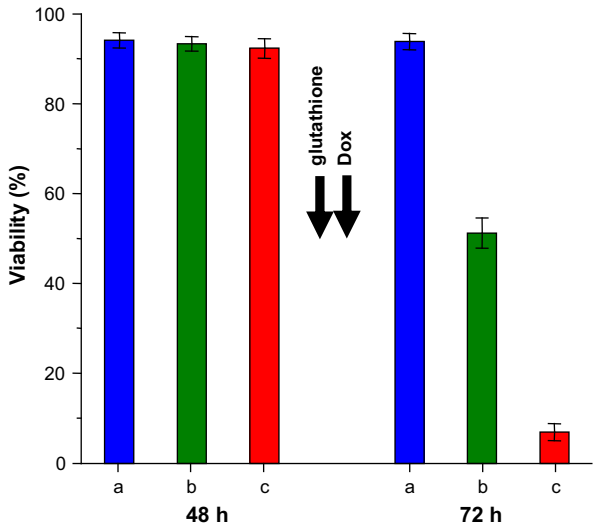

Fig. 18. Viability of HeLa cells after incubation for 48 and 72 h in different systems: (a) control; (b) Dox-loaded nanogels, where glutathione was added after 48 h incubation to release Dox from Dox-loaded nanogels; (c) control, where free Dox was added after 48 h incubation. Reprinted with permission from Ref. [80]. Copyright 2007 American Chemical Society.

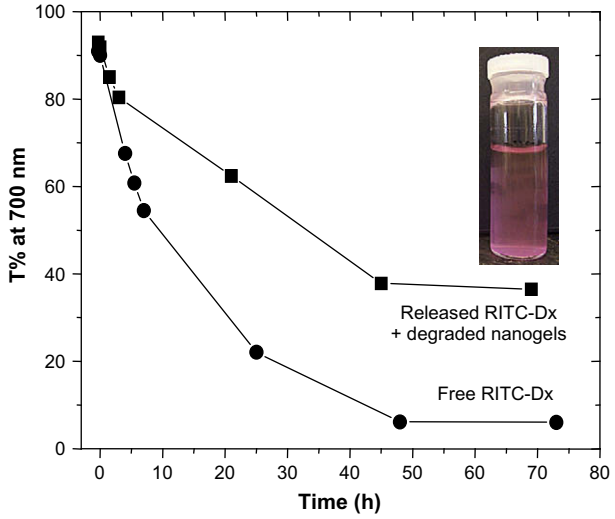

Fig. 19. Transmittance at 700 nm vs. time for a mixture of RITC-dextran released from nanogels upon degradation in the presence of glutathione, compared with that of free RITC-Dex in PBS buffer. Digital image of the final dispersions showing the precipitation of aggregates (inset). Reprinted with permission from Ref. [82]. Copyright 2007 American Chemical Society.

molecules with ConA, resulting in an increase in the turbidity of the mixtures. Large aggregates were finally precipitated, as observed in the inset of Fig. 19. These results clearly imply that carbohydrate drugs released from nanogels upon degradation interact with the targeted proteins.

9. Chain extension, bioconjugation, and cellular uptake of nanogels

9.1. ATRP chain extension with polystyrene

An advantage of using ATRP is the preservation of halogen chain end functionality in the resulting polymers. This halide functionality enables further chain extension and/or modification and functionalization of the polymers with biorelated molecules. This section describes ATRP chain extension (*ce*) of nanogel macroinitiators with polystyrene as well as degradation of nanogel-*ce*-PS and micellization of amphiphilic degraded POEOMA-b-PS in water (Fig. 20) [78].

The chain extension of ATRP-nanogel macroinitiators with polystyrene displayed first-order kinetics and conversion reached 30% after 19 h. The final copolymer was degraded in the presence of Bu_3P in THF for HPLC analysis. As seen in Fig. 21a, there is no significant amount of POEOMA300 macroinitiators left in the reaction mixture, indicating that most POEOMA300 chains were functionalized with a bromine end group and capable of chain extension. The degraded POEOMA300-b-PS block copolymers self-assembled to form stable uniform spherical micellar particles consisting of a PS core and POEOMA300 corona.

Fig. 21b. No aggregates were observed. The particle size was 226 ± 48 nm in diameter, as measured by TEM, as compared with 445 ± 30 nm by DLS. These results confirm the successful chain extension of PS from the active Br-functionality in the POEOMA300 nanogels.

9.2. Bioconjugation of nanogels

The preparation of OH-functionalized POEOMA nanogels by using a functionalized ATRP initiator or introducing HEA or HEMA during an active inverse miniemulsion ATRP of OEOMA was described in Section 4. The resulting OH-functionalized nanogels were reacted with biotin (Vitamin H) using a carbodiimide coupling reaction, resulting in the formation of biotin-functionalized nanogels [80]. Avidin/2-(4-hydroxyphenylazo)benzoic acid (HABA) binding assay and OFM was used to evaluate the bioavailability of biotin present in the nanogels to its protein receptor. Fig. 22a shows the results from avidin/HABA binding assay. The addition of biotin-functionalized nanogels to an avidin/HABA solution resulted in a sharp decrease in the absorbance at 500 nm from 0.79 to 0.27,

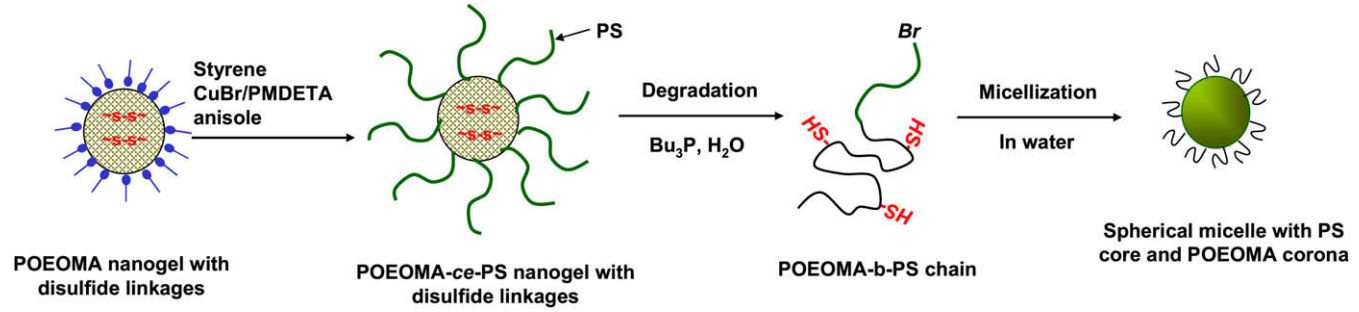

Fig. 20. An illustration of ATRP chain extension with polystyrene from ATRP-nanogels, degradation of nanogel-*ce*-PS, and micellization of amphiphilic POEOMA-b-PS in water.

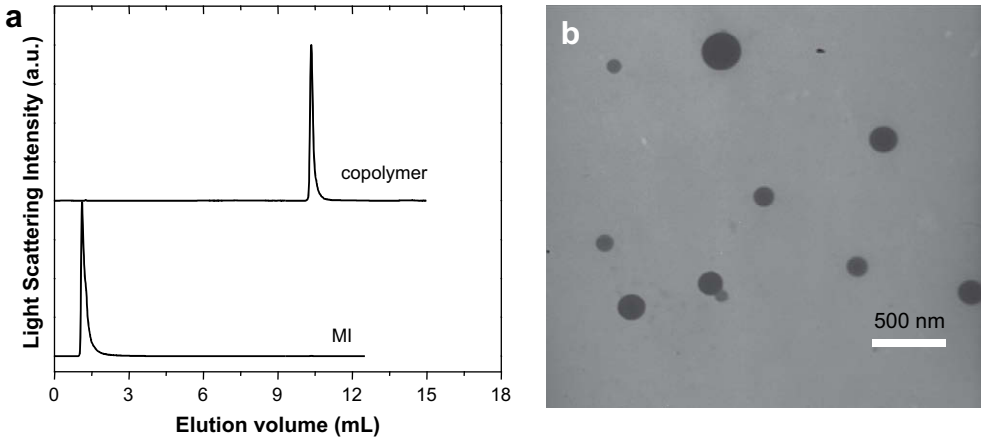

Fig. 21. HPLC chromatograms of POEOMA300 macroinitiator (MI) and POEOMA300-block-PS (a), and TEM image of spherical micelles consisting of PS core and POEOMA300 corona formed from self-assembly of degraded POEOMA300-block-PS in water (b). Conditions for chain extension of POEOMA300 nanogel macroinitiators with PS in anisole at 90 °C: $[styrene]_0/[CuBr]_0/[PMDETA]_0 = 1605/1/1$ and styrene/anisole = 50/50 v/v. Reprinted with permission from Ref. [78]. Copyright 2006 American Chemical Society.

indicating that the biotin molecules in the nanogels competitively bind to avidin, and replace HABA molecules. Using the calibration plot determined for free biotin in water [215], the amount of biotin in the nanogels was calculated to be 16.7 nmol/mg polymer, corresponding to 142,000 biotin molecules available in each nanogel particle, based on the diameter of nanogels in water (310 nm).

The biotin-functionalized nanogels were mixed with fluorescein isothiocyanate-labeled avidin (FITC–avidin) in PBS buffer for OFM analysis, resulting in the formation of aggregates of avidin–biotin-nanogels. As shown in Fig. 22b, the presence of distinct bright spots on the dark background indicate the formation of complex of biotin-nanogels with FITC-labeled avidin. The large fluorescent spots may indicate the formation of large aggregates since each avidin has four binding pockets to biotin. Formation of similar aggregates of avidin and biotin-functionalized polymers was also found in literature [215–217].

Nanogels were also functionalized with oligopeptides, in particular amino-terminated glycine-arginine-glycine aspartic acid-serine (GRGDS-NH_2), a short fibronectin peptide known to promote integrin-mediated cell adhesion. For this, OH groups in POEOMA nanogels were converted to the corresponding carboxylic acids in a high yield by reacting with succinic anhydride in DMF. HOOC-POEOMA nanogels were subsequently conjugated with GRGDS-NH_2 via carbodiimide-mediated reaction, producing GRGDS-conjugated POEOMA nanogels, confirmed by ^{1}H NMR spectroscopy [102].

9.3. Cellular internalization of nanogels

Cell internalization is one of the key steps for effective delivery and controllable release of encapsulated molecules. MC3T3-E1 (subclone 4) mouse calvarial osteoprogenitor cells were cultured in the presence of pure and GRGDS-containing FITC-Dex loaded POEOMA nanogels. The biocompatible POEOMA nanosized gels entered cells via clathrin-mediated endocytosis [218]. Flow cytometry was used to quantify cellular uptake of FITC-Dex loaded nanogels at different incubation time. Fig. 23 presents count vs. intensity plots and an illustration of the uniform network of bioconjugated nanogels with cell-adhesive GRGDS oligopeptide. The internalization of pure FITC-Dex loaded nanogels was 62% after 45 min of incubation and reached up to 82% after 90 min (a). Using similar experimental conditions, cellular uptake of GRGDS-conjugated FITC-Dex loaded POEOMA nanogels increased to 95% after 45 min and nearly complete internalization was obtained after 90 min, with a shift toward higher fluorescence intensity (b). Bioactive molecules may promote cell-nanogels interactions leading to efficient cellular

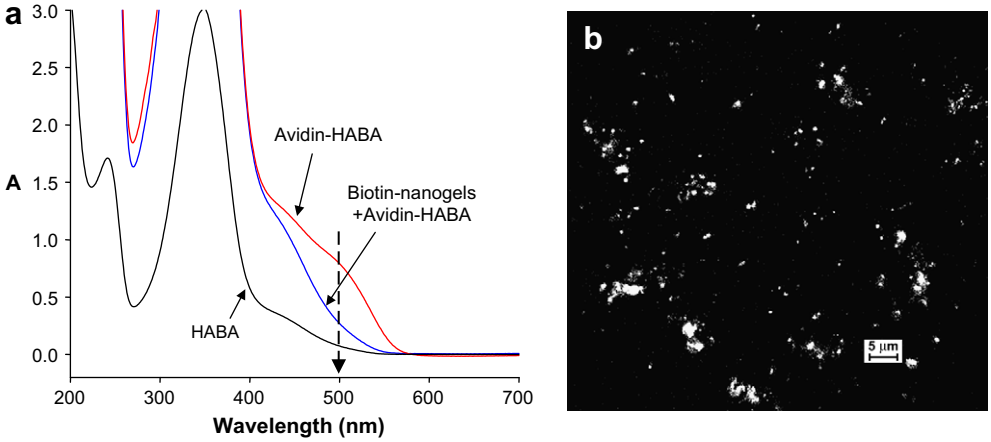

Fig. 22. UV spectra of HABA and avidin–HABA complex before and after addition of biotin-nanogels in PBS buffer (a) and OFM image of FITC–avidin–biotin-nanogel conjugates (b). Scale bar = 5 μm. Reprinted with permission from Ref. [80]. Copyright 2007 American Chemical Society.

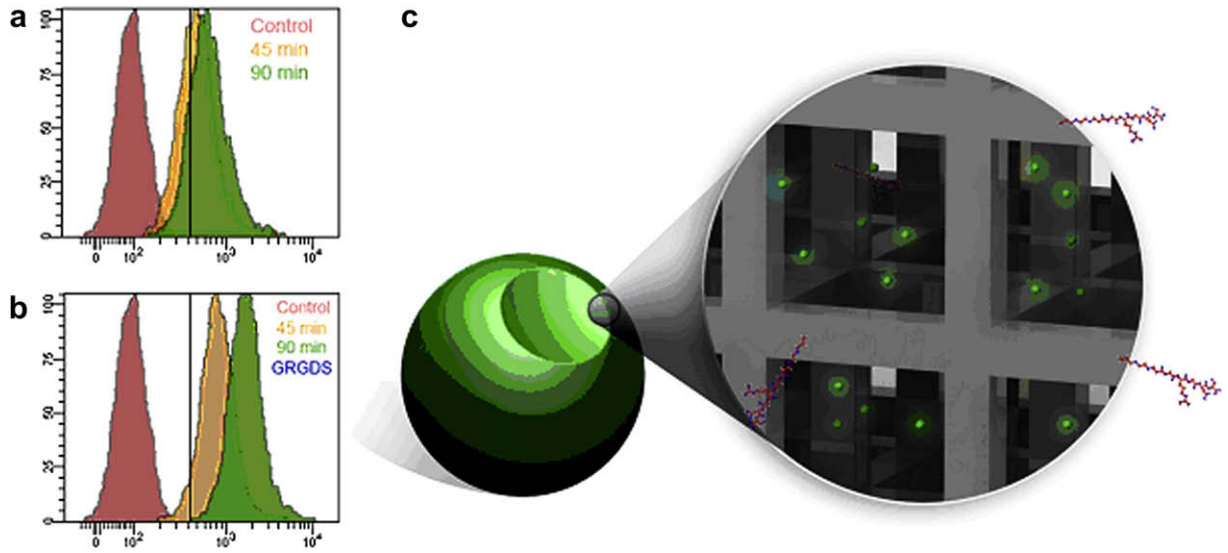

Fig. 23. Flow cytometry results illustrating fluorescence intensity for FITC-Dextran-loaded POEOMA nanogels with (b) and without (a) bioconjugation of GRGDS. Encapsulation of FITC-Dextran molecules inside of the uniform peptide-modified POEOMA network (grey bars) is illustrated (c). [195] (Reprinted with permission from Ref. [195]. Copyright 2009 American Chemical Society).

uptake. These results confirmed that nanogels prepared by ATRP in inverse miniemulsion are endocytosed in cells and are applicable as drug delivery devices.

10. Fabrication of nanogels for advanced DDS

The development of hybrid polymeric scaffolds with nanosized materials has offered precise control over the release of biomolecules [219]. Novel nanostructured hybrid drug delivery scaffolds were prepared by a combination of ATRP and conventional free-radical polymerization (FRP). OH-functionalized nanogels prepared by AGET ATRP in inverse miniemulsion were first modified with polymerizable methacrylate groups using two approaches. One approach involves the reaction of OH groups with methacrylate anhydride. The other approach involves the reaction of OH groups with dithiopropionic acid using a coupling chemistry, followed by reaction with HEMA, yielding HEMA-disulfide-functionalized nanogels. The resulting polymerizable nanogels functionalized with disulfide-HEMA were photo-copolymerized with methacrylated hyaluronic acid macromonomer, producing biodegradable 3D hydrogels, in which nanogels were covalently incorporated. Upon degradation, the disulfides were cleaved to release nanogels from hydrogels. These novel hybrid polymeric scaffolds are very promising for tissue engineering applications. They enable control over release of sequential encapsulated biomolecules from nanogels such as multiple growth factors, which is required at distinct stages in the development of important regenerative processes in biology and medicine [219].

Recently, injectable biomaterials have been the important subject of much research in both fields of drug delivery and tissue engineering, largely due to the minimally invasive nature with which they can be delivered. A novel *in-situ* nanostructured polymeric 3D DDS was developed by mixing biodegradable thiolated hyaluronic acid (HA-SH) with hydrolyzable acrylated-POEOMA-co-PHEMA nanogels (ACRL-nanogels) prepared by AGET ATRP. As shown in Fig. 24, gelation was achieved via a Michael addition reaction, leading to a chemically crosslinked hybrid scaffold under physiological conditions (pH = 7.4, 37 °C). This novel injectable

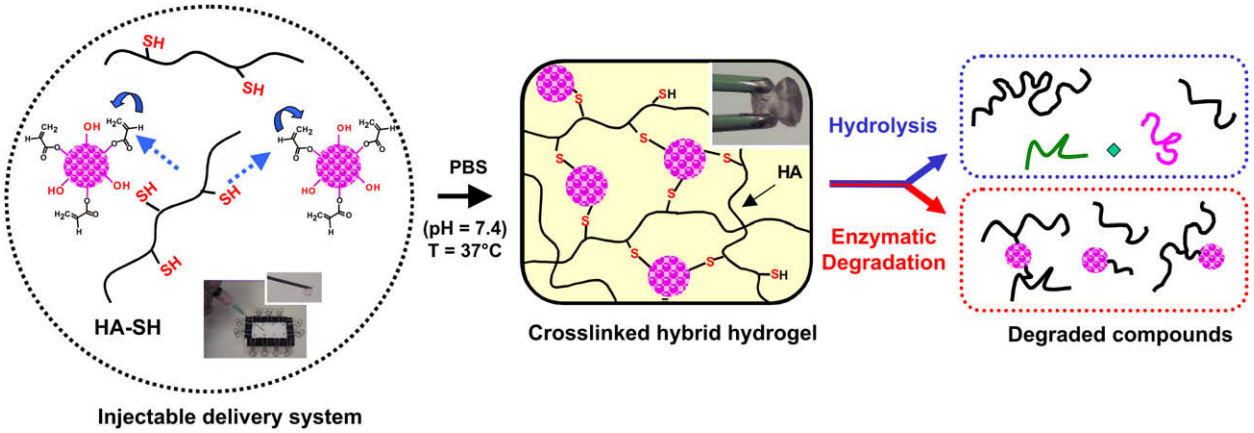

Fig. 24. Injectable nanostructured DDS prepared by a combination of ATRP and Michael addition reaction. Employing both water-soluble thiolated HA and ACRLnanogels formed a biodegradable chemical network under physiological conditions. The nanostructured DDS is resorbable through hydrolysis and enzymatic degradation resulting in water-soluble components.

biodegradable scaffold is useful in both tissue engineering and drug delivery applications. In addition, this approach offers an additional unique advantage for the mechanism of scaffold degradation. *In vivo* applications, matrix resorption can occur via two independent pathways; hydrolytic (nanogels) and enzymatic (hyaluronic acid backbone).

11. Summary and outlook

A versatile method combining ATRP, inverse miniemulsion polymerization, and disulfide–thiol exchange enabled preparation and functionalization of well-defined biodegradable nanogels with some useful features for targeted drug delivery applications. In the absence of the difunctional crosslinker, well-controlled water-soluble and hydrophilic homo and block copolymers with low polydispersity ($M_w/M_n < 1.3$) were produced as stable submicron-sized particles with diameter from 100 to 300 nm and narrow size distribution. In the presence of a disulfide- or polyester-functionalized crosslinker, crosslinked biodegradable nanogels were prepared. They were non-toxic when exposed to cells.

Several methods were explored for loading various water-soluble biomolecules and inorganic nanoparticles into the nanogels at high loading levels and high yield. Fluorescent dyes, AuNPs, and anticancer drugs were incorporated by physical loading, high molecular weight carbohydrates and proteins by *in-situ* physical incorporation, and star branched polymeric nanoparticles by *in-situ* covalent incorporation. The nanogels crosslinked with polyester or disulfide linkages were biodegraded either in aqueous media or in the presence of biocompatible reducing agents such as glutathione, naturally present within cells. Upon degradation, encapsulated anticancer drugs such as Dox were released in a controlled manner to kill cancer cells. Carbohydrate drugs released from nanogels were bound to lectin such as ConA. The nanogels preserved bromine chain end functionality that enabled further chain extension and modification and functionalization of the nanogels with biorelated molecules. Functional nanogels were prepared by copolymerization with functional monomers or through the use of functional ATRP initiators. They were further functionalized with biorelated molecules, such as cell-adhesive peptides, targeting proteins and antibodies, resulting in the formation of nanogel bioconjugates. Finally, ATRP-nanogels had higher swelling ratios, better colloidal stability, and more controlled degradation than FRP-nanogels. These overall results suggest that well-defined functional nanogels may have potential as carriers for controlled drug delivery scaffolds to target specific cells.

Future design and development of effective microgel/nanogel-based DDS utilizing CRP methods (not only ATRP) for *in vivo* applications to target cancer cells require a higher degree of control over properties. Targeted dimensions are in the range of 100 nm diameter, with a rapid environmental response for enhanced loading level, novel functionality for further bioconjugation, and biodegradability for sustained release of drugs. CRP in inverse microemulsion polymerization could produce nanogels with diameter less than 50 nm and with a uniform crosslinked network for better swelling. Appropriate selection of environmentally responsive water-soluble and water-swellable monomers will enable developing biomaterials responsive to external stimuli. In addition, introduction of acid-labile degradation linkages with/or without disulfide linkages will allow DDS to be effectively degraded in targeted cancer cells.

Acknowledgements

Authors thank Dr. Daniel J. Siegwart, Dr. Chuanbing Tang, Fabien Perineau, Hongchen Dong, Rui Zhang, Gizelle Sherwood, Dr. Haifeng Gao, Dr. Abiraman Srinivasan and Dr. James Spanswick for their support and discussions. JKO thanks Natural Sciences and Engineering Research Council (NSERC) of Canada for a prestigious postdoctoral fellowship during his 2 years residence at Carnegie Mellon University. KM acknowledges support from NSF DMR 05-49353.

References

[1] Zhang H, Mardyani S, Chan WCW, Kumacheva E. Biomacromolecules 2006;7:1568.
[2] Jung T, Kamm W, Breitenbach A, Kaiserling E, Xiao JX, Kissel T. Eur J Pharm Biopharm 2000;50:147.
[3] Raemdonck K, Demeester J, De Smedt S. Soft Matter 2009;5:707.
[4] Oh JK, Drumright R, Siegwart DJ, Matyjaszewski K. Prog Polym Sci 2008;33:448.
[5] Hamidi M, Azadi A, Rafiei P. Adv Drug Deliv Rev 2008;60:1638.
[6] Vert M. Prog Polym Sci 2007;32:755.
[7] Lee KY, Yuk SH. Prog Polym Sci 2007;32:669.
[8] Park JH, Lee S, Kim J-H, Park K, Kim K, Kwon IC. Prog Polym Sci 2008;33:113.
[9] Wong SY, Pelet JM, Putnam D. Prog Polym Sci 2007;32:799.
[10] Discher DE, Ortiz V, Srinivas G, Klein ML, Kim Y, Christian D, et al. Prog Polym Sci 2007;32:838.
[11] Hoffman AS, Stayton PS. Prog Polym Sci 2007;32:922.
[12] Pasut G, Veronese FM. Prog Polym Sci 2007;32:933.
[13] Dandu R, Ghandehari H. Prog Polym Sci 2007;32:1008.
[14] Kabanov AV, Gendelman HE. Prog Polym Sci 2007;32:1054.
[15] Martens PJ, Bryant SJ, Anseth KS. Biomacromolecules 2003;4:283.
[16] Eichenbaum KD, Thomas AA, Eichenbaum GM, Gibney BR, Needham D, Kiser PF. Macromolecules 2005;38:10757.
[17] Huang X, Lowe TL. Biomacromolecules 2005;6:2131.
[18] Rice MA, Sanchez-Adams J, Anseth KS. Biomacromolecules 2006;7:1968.
[19] Leemhuis M, Kruijtzer JAW, Van Nostrum CF, Hennink WE. Biomacromolecules 2007;8:2943.
[20] Muggli DS, Burkoth AK, Keyser SA, Lee HR, Anseth KS. Macromolecules 1998;31:4120.
[21] Plunkett KN, Berkowski KL, Moore JS. Biomacromolecules 2005;6:632.
[22] Kim S, Healy KE. Biomacromolecules 2003;4:1214.
[23] Levesque SG, Shoichet MS. Bioconjug Chem 2007;18:874.
[24] Perez P, Plieva F, Gallardo A, San Roman J, Aguilar MR, Morfin I, et al. Biomacromolecules 2008;9:66.
[25] Kitamura T, Matsumoto A. Macromolecules 2007;40:6143.
[26] Nayak S, Lyon LA. Angew Chem Int Ed 2004;43:6706.
[27] Murthy N, Thng YX, Schuck S, Xu MC, Frechet JMJ. J Am Chem Soc 2002;124:12398.
[28] Themistou E, Patrickios CS. Macromolecules 2007;40:5231.
[29] Kaihara S, Matsumura S, Fisher JP. Macromolecules 2007;40:7625.
[30] Li Y, Du W, Sun G, Wooley KL. Macromolecules 2008;41:6605.
[31] Chan Y, Wong T, Byrne F, Kavallaris M, Bulmus V. Biomacromolecules 2008;9:1826.
[32] Shi L, Khondee S, Linz TH, Berkland C. Macromolecules 2008;41:6546.
[33] Zhang L, Bernard J, Davis TP, Barner-Kowollik C, Stenzel MH. Macromol Rapid Commun 2008;29:123.
[34] Neugebauer D, Rydz J, Goebel I, Dacko P, Kowalczuk M. Macromolecules 2007;40:1767.
[35] Li Q, Wang J, Shahani S, Sun DDN, Sharma B, Elisseeff JH, et al. Biomaterials 2006;27:1027.
[36] Du J-Z, Sun T-M, Weng S-Q, Chen X-S, Wang J. Biomacromolecules 2007;8:3375.
[37] Aliyar HA, Hamilton PD, Ravi N. Biomacromolecules 2005;6:204.
[38] Ulbrich K, Etrych T, Chytil P, Jelinkova M, Rihova B. J Control Release 2003;87:33.
[39] Bae Y, Fukushima S, Harada A, Kataoka K. Angew Chem Int Ed 2003;42:4640.
[40] Rolland JP, Maynor BW, Euliss LE, Exner AE, Denison GM, DeSimone JM. J Am Chem Soc 2005;127:10096.
[41] Yeh J, Ling Y, Karp JM, Gantz J, Chandawarkar A, Eng G, et al. Biomaterials 2006;27:5391.
[42] Franzesi GT, Ni B, Ling Y, Khademhosseini A. J Am Chem Soc 2006;128:15064.
[43] Zhang H, Tumarkin E, Sullan RMA, Walker GC, Kumacheva E. Macromol Rapid Commun 2007;28:527.
[44] Zhang H, Tumarkin E, Peerani R, Nie Z, Sullan RMA, Walker GC, et al. J Am Chem Soc 2006;128:12205.
[45] Mitra S, Gaur U, Ghosh PC, Maitra AN. J Control Release 2001;74:317.
[46] Lee H, Mok H, Lee S, Oh Y-K, Park TG. J Control Release 2007;119:245.
[47] Wang L-Y, Ma G-H, Su Z- G. J Control Release 2005;106:62.
[48] Zhou Q-Z, Wang L-Y, Ma G-H, Su Z-G. J Colloid Interface Sci 2007;311:118.
[49] Shen X, Zhang L, Jiang X, Hu Y, Guo J. Angew Chem Int Ed 2007;46:7104.
[50] Zhang H, Oh M, Allen C, Kumacheva E. Biomacromolecules 2004;5:2461.
[51] Horak D, Lednicky F, Petrovsky E, Kapicka A. Macromol Mater Eng 2004;289:341.
[52] Horak D, Rittich B, Spanova A, Benes MJ. Polymer 2005;46:1245.
[53] Kim J, Nayak S, Lyon LA. J Am Chem Soc 2005;127:9588.
[54] Thornton PD, McConnell G, Ulijn RV. Chem Commun 2005:5913.

[55] Ulijn RV, Bibi N, Jayawarna V, Thornton PD, Todd SJ, Mart RJ, et al. Mater Today 2007;10:40.
[56] Matyjaszewski K, Davis TP. Handbook of radical polymerization. John Wiley & Sons Ltd; 2002.
[57] Davis KA, Matyjaszewski K. Adv Polym Sci 2002;159:1.
[58] Coessens V, Pintauer T, Matyjaszewski K. Prog Polym Sci 2001;26:337.
[59] Braunecker WA, Matyjaszewski K. Prog Polym Sci 2007;32:93.
[60] Matyjaszewski K, Gaynor S, Greszta D, Mardare D, Shigemoto T. J Phys Org Chem 1995;8:306.
[61] Matyjaszewski K. J Phys Org Chem 1995;8:197.
[62] Ide N, Fukuda T. Macromolecules 1997;30:4268.
[63] Shim SE, Oh S, Chang YH, Jin M-J, Choe S. Polymer 2004;45:4731.
[64] Tsarevsky NV, Matyjaszewski K. Macromolecules 2005;38:3087.
[65] Li W, Gao H, Matyjaszewski K. Macromolecules 2009;42:927.
[66] Min K, Gao H, Yoon JA, Wu W, Kowalewski T, Matyjaszewski K. Macromolecules 2009;42:1597.
[67] Gao H, Matyjaszewski K. Prog Polym Sci 2009;34:317.
[68] Gao H, Miasnikova A, Matyjaszewski K. Macromolecules 2008;41:7843.
[69] Gao H, Min K, Matyjaszewski K. Macromolecules 2007;40:7063.
[70] Huang J, Cusick B, Pietrasik J, Wang L, Kowalewski T, Lin Q, et al. Langmuir 2007;23:241.
[71] An Z, Shi Q, Tang W, Tsung C-K, Hawker CJ, Stucky GD. J Am Chem Soc 2007;129:14493.
[72] Wang J-S, Matyjaszewski K. Macromolecules 1995;28:7901.
[73] Wang J-S, Matyjaszewski K. J Am Chem Soc 1995;117:5614.
[74] Chan Y, Bulmus V, Zareie MH, Byrne FL, Barner L, Kavallaris M. J Control Release 2006;115:197.
[75] Poly J, Wilson DJ, Destarac M, Taton D. Macromol Rapid Commun 2008;29:1965.
[76] Rieger J, Grazon C, Charleux B, Alaimo D, Jerome C. J Polym Sci Part A Polym Chem 2009;47:2373.
[77] Lutz J-F, Boerner HG. Prog Polym Sci 2008;33:1.
[78] Oh JK, Tang C, Gao H, Tsarevsky NV, Matyjaszewski K. J Am Chem Soc 2006;128:5578.
[79] Oh JK, Perineau F, Matyjaszewski K. Macromolecules 2006;39:8003.
[80] Oh JK, Siegwart DJ, Lee H-i, Sherwood G, Peteanu L, Hollinger JO, et al. J Am Chem Soc 2007;129:5939.
[81] Oh JK, Dong H, Zhang R, Matyjaszewski K, Schlaad H. J Polym Sci Part A Polym Chem 2007;45:4764.
[82] Oh JK, Siegwart DJ, Matyjaszewski K. Biomacromolecules 2007;8:3326.
[83] Antonietti M, Landfester K. Prog Polym Sci 2002;27:689.
[84] Tsarevsky NV, Matyjaszewski K. Macromolecules 2002;35:9009.
[85] Tsarevsky NV, Bernaerts KV, Dufour B, Du Prez FE, Matyjaszewski K. Macromolecules 2004;37:9308.
[86] Landfester K, Willert M, Antonietti M. Macromolecules 2000;33:2370.
[87] Kriwet B, Walter E, Kissel T. J Control Release 1998;56:149.
[88] Sun Q, Deng Y. J Am Chem Soc 2005;127:8274.
[89] Sankar C, Rani M, Srivastava AK, Mishra B. Pharmazie 2001;56:223.
[90] Marie E, Rothe R, Antonietti M, Landfester K. Macromolecules 2003;36:3967.
[91] Wormuth K. J Colloid Interface Sci 2001;241:366.
[92] Xu ZZ, Wang CC, Yang WL, Deng YH, Fu SK. J Magn Magn Mater 2004;277:136.
[93] Voorn DJ, Ming W, Van Herk AM. Macromolecules 2006;39:2137.
[94] Dowding PJ, Vincent B, Williams E. J Colloid Interface Sci 2000;221:268.
[95] Owens III DE, Jian Y, Fang JE, Slaughter BV, Chen Y-H, Peppas NA. Macromolecules 2007;40:7306.
[96] Missirlis D, Tirelli N, Hubbell JA. Langmuir 2005;21:2605.
[97] Rubio-Retama J, Tamimi FM, Heinrich M, Lopez-Cabarcos E. Langmuir 2007;23:8538.
[98] Zhang Y, Zhu W, Ding J. J Biomed Mater Res Part A 2005;75A:342.
[99] Murthy N, Xu M, Schuck S, Kunisawa J, Shastri N, Frechet JMJ. Proc Natl Acad Sci U S A 2003;100:4995.
[100] Goh SL, Murthy N, Xu M, Frechet JMJ. Bioconjug Chem 2004;15:467.
[101] Oh JK, Perineau F, Charleux B, Matyjaszewski K. J Polym Sci Part A Polym Chem 2009;47:1771.
[102] Siegwart DJ, Oh JK, Gao H, Bencherif SA, Perineau F, Bohaty AK, et al. Macromol Chem Phys 2008;209:2179.
[103] Qi G, Jones CW, Schork FJ. Macromol Rapid Commun 2007;28:1010.
[104] Candau F. In: Lovell P, El-Aasser MS, editors. Emulsion polymerization and emulsion polymers. West Sussex, England: John Wiley & Sons Ltd; 1997. p. 723.
[105] Nagarajan R, Wang C-C. Langmuir 2000;16:5243.
[106] Braun O, Selb J, Candau F. Polymer 2001;42:8499.
[107] Fernandez VVA, Tepale N, Sanchez-Diaz JC, Mendizabal E, Puig JE, Soltero JFA. Colloid Polym Sci 2006;284:387.
[108] Juranicova V, Kawamoto S, Fujimoto K, Kawaguchi H, Barton J. Angew Makromol Chem 1998;258:27.
[109] Barton J. Macromol Symp 2002;179:189.
[110] Renteria M, Munoz M, Ochoa JR, Cesteros LC, Katime I. J Polym Sci Part A Polym Chem 2005;43:2495.
[111] Kaneda I, Sogabe A, Nakajima H. J Colloid Interface Sci 2004;275:450.
[112] Gupta Ajay K, Wells S. IEEE Trans Nanobiosci 2004;3:66.
[113] Deng Y, Wang L, Yang W, Fu S, Elaissari A. J Magn Magn Mater 2003;257:69.
[114] Gaur U, Sahoo SK, De TK, Ghosh PC, Maitra A, Ghosh PK. Int J Pharm 2000;202:1.
[115] Bharali DJ, Sahoo SK, Mozumdar S, Maitra A. J Colloid Interface Sci 2003;258:415.
[116] McAllister K, Sazani P, Adam M, Cho MJ, Rubinstein M, Samulski RJ, et al. J Am Chem Soc 2002;124:15198.
[117] Craparo EF, Cavallaro G, Bondi ML, Mandracchia D, Giammona G. Biomacromolecules 2006;7:3083.
[118] Gao D, Xu H, Philbert MA, Kopelman R. Angew Chem Int Ed 2007;46:2224.
[119] Gao D, Agayan RR, Xu H, Philbert MA, Kopelman R. Nano Lett 2006;6:2383.
[120] Das M, Mardyani S, Chan WCW, Kumacheva E. Adv Mater 2006;18:80.
[121] Thronton PD, Mart RJ, Ulijn RV. Adv Mater 2007;19:1252.
[122] Kim J, Serpe MJ, Lyon LA. Angew Chem Int Ed 2005;44:1333.
[123] Patten TE, Xia J, Abernathy T, Matyjaszewski K. Science 1996;272:866.
[124] Kamigaito M, Ando T, Sawamoto M. Chem Rev 2001;101:3689.
[125] Matyjaszewski K, Xia J. Chem Rev 2001;101:2921.
[126] Tsarevsky NV, Matyjaszewski K. Chem Rev 2007;107:2270.
[127] Sheiko SS, Sumerlin BS, Matyjaszewski K. Prog Polym Sci 2008;33:759.
[128] Yagci Y, Tasdelen MA. Prog Polym Sci 2006;31:1133.
[129] Hadjichristidis N, Iatrou H, Pitsikalis M, Mays J. Prog Polym Sci 2006;31:1068.
[130] Beers KL, Gaynor SG, Matyjaszewski K, Sheiko SS, Moeller M. Macromolecules 1998;31:9413.
[131] Matyjaszewski K. Polym Int 2003;52:1559.
[132] Pyun J, Matyjaszewski K. Chem Mater 2001;13:3436.
[133] Pyun J, Kowalewski T, Matyjaszewski K. Macromol Rapid Commun 2003;24:1043.
[134] Matyjaszewski K, Ziegler MJ, Arehart SV, Greszta D, Pakula T. J Phys Org Chem 2000;13:775.
[135] Nicolas J, Mantovani G, Haddleton DM. Macromol Rapid Commun 2007;28:1083.
[136] Lele BS, Murata H, Matyjaszewski K, Russell AJ. Biomacromolecules 2005;6:3380.
[137] Chen G, Huynh D, Felgner PL, Guan Z. J Am Chem Soc 2006;128:4298.
[138] Heredia KL, Tolstyka ZP, Maynard HD. Macromolecules 2007;40:4772.
[139] Broyer RM, Quaker GM, Maynard HD. J Am Chem Soc 2008;130:1041.
[140] Le Droumaguet B, Velonia K. Angew Chem Int Ed 2008;47:6263.
[141] Kopping JT, Tolstyka ZP, Maynard HD. Macromolecules 2007;40:8593.
[142] Loschonsky S, Couet J, Biesalski M. Macromol Rapid Commun 2008;29:309.
[143] Carlmark A, Malmstroem E. J Am Chem Soc 2002;124:900.
[144] Bontempo D, Masci G, De Leonardis P, Mannina L, Capitani D, Crescenzi V. Biomacromolecules 2006;7:2154.
[145] Ostmark E, Harrisson S, Wooley Karen L, Malmstrom Eva E. Biomacromolecules 2009;8:1138.
[146] Ifuku S, Kadla JF. Biomacromolecules 2008;9:3308.
[147] Sui X, Yuan J, Zhou M, Zhang J, Yang H, Yuan W, et al. Biomacromolecules 2008;9:2615.
[148] Yan L, Ishihara K. J Polym Sci Part A Polym Chem 2008;46:3306.
[149] Xu P, Van Kirk EA, Murdoch WJ, Zhan Y, Isaak DD, Radosz M, et al. Biomacromolecules 2006;7:829.
[150] Jiang X, Ge Z, Xu J, Liu H, Liu S. Biomacromolecules 2007;8:3184.
[151] Licciardi M, Tang Y, Billingham NC, Armes SP, Lewis AL. Biomacromolecules 2005;6:1085.
[152] Buetuen V, Liu S, Weaver JVM, Bories-Azeau X, Cai Y, Armes SP. React Funct Polym 2006;66:157.
[153] Jiang J, Tong X, Morris D, Zhao Y. Macromolecules 2006;39:4633.
[154] Joralemon MJ, Smith NL, Holowka D, Baird B, Wooley KL. Bioconjug Chem 2005;16:1246.
[155] Sun X, Rossin R, Turner JL, Becker ML, Joralemon MJ, Welch MJ, et al. Biomacromolecules 2005;6:2541.
[156] Wang X-S, Dykstra TE, Salvador MR, Manners I, Scholes GD, Winnik MA. J Am Chem Soc 2004;126:7784.
[157] Wang M, Oh JK, Dykstra TE, Lou X, Scholes GD, Winnik MA. Macromolecules 2006;39:3664.
[158] Wang M, Dykstra TE, Lou X, Salvador MR, Scholes GD, Winnik MA. Angew Chem Int Ed 2006;45:2221.
[159] Wang M, Felorzabihi N, Guerin G, Haley JC, Scholes GD, Winnik MA. Macromolecules 2007;40:6377.
[160] Neugebauer D, Zhang Y, Pakula T, Sheiko SS, Matyjaszewski K. Macromolecules 2003;36:6746.
[161] Matyjaszewski K, Miller PJ, Shukla N, Immaraporn B, Gelman A, Luokala BB, et al. Macromolecules 1999;32:8716.
[162] Huang J, Koepsel RR, Murata H, Wu W, Lee SB, Kowalewski T, et al. Langmuir 2008;24:6785.
[163] Huang J, Murata H, Koepsel RR, Russell AJ, Matyjaszewski K. Biomacromolecules 2007;8:1396.
[164] Oh JK. J Polym Sci Part A Polym Chem 2008;46:6983.
[165] Cunningham MF. Prog Polym Sci 2008;33:365.
[166] Qiu J, Charleux B, Matyjaszewski K. Prog Polym Sci 2001;26:2083.
[167] Matyjaszewski K, Patten TE, Xia J. J Am Chem Soc 1997;119:674.
[168] Qiu J, Matyjaszewski K, Thouin L, Amatore C. Macromol Chem Phys 2000;201:1625.

[169] Matyjaszewski K, Tsarevsky NV, Braunecker WA, Dong H, Huang J, Jakubowski W, et al. Macromolecules 2007;40:7795.
[170] Matyjaszewski K, Paik H-j, Zhou P, Diamanti SJ. Macromolecules 2001;34:5125.
[171] Jakubowski W, Matyjaszewski K. Macromolecules 2005;38:4139.
[172] Jakubowski W, Matyjaszewski K. Angew Chem Int Ed 2006;45:4482.
[173] Min K, Jakubowski W, Matyjaszewski K. Macromol Rapid Commun 2006;27:594.
[174] Kwiatkowski P, Jurczak J, Pietrasik J, Jakubowski W, Mueller L, Matyjaszewski K. Macromolecules 2008;41:1067.
[175] Oh JK, Matyjaszewski K. J Polym Sci Part A Polym Chem 2006;44:3787.
[176] Oh JK, Min K, Matyjaszewski K. Macromolecules 2006;39:3161.
[177] Min K, Matyjaszewski K. Macromolecules 2005;38:8131.
[178] Min K, Gao H, Matyjaszewski K. J Am Chem Soc 2006;128:10521.
[179] Min K, Gao H, Matyjaszewski K. J Am Chem Soc 2005;127:3825.
[180] Min K, Oh JK, Matyjaszewski K. J Polym Sci Part A Polym Chem 2007;45:1413.
[181] Bombalski L, Min K, Dong H, Tang C, Matyjaszewski K. Macromolecules 2007;40:7429.
[182] Min K, Yu S, Lee H-i, Mueller L, Sheiko SS, Matyjaszewski K. Macromolecules 2007;40:6557.
[183] Li W, Min K, Matyjaszewski K, Stoffelbach F, Charleux B. Macromolecules 2008;41:6387.
[184] Min K, Matyjaszewski K. Macromolecules 2007;40:7217.
[185] Brannon-Peppas L. J Control Release 2000;66:321.
[186] Tsarevsky NV, Pintauer T, Matyjaszewski K. Macromolecules 2004;37:9768.
[187] Tsarevsky NV, Matyjaszewski K. ACS Symp Ser 2006;937:79.
[188] Sarbu T, Lin K-Y, Spanswick J, Gil RR, Siegwart DJ, Matyjaszewski K. Macromolecules 2004;37:9694.
[189] Tsarevsky NV, Sumerlin BS, Matyjaszewski K. Macromolecules 2005;38:3558.
[190] Heredia KL, Bontempo D, Ly T, Byers JT, Halstenberg S, Maynard HD. J Am Chem Soc 2005;127:16955.
[191] Bontempo D, Maynard HD. J Am Chem Soc 2005;127:6508.
[192] Bencherif SA, Sheehan JA, Hollinger JO, Walker LM, Matyjaszewski K, Washburn NR. J Biomed Mater Res A 2008;90A:142.
[193] Bencherif SA, Srinivasan A, Sheehan JA, Gayathri C, Gil R, Walker LM, et al. Acta Biomater 2009;5:1872.
[194] Shinoda H, Matyjaszewski K. Macromolecules 2001;34:6243.
[195] Siegwart DJ, Srinivasan A, Bencherif SA, Karunanidhi A, Oh JK, Vaidya S, et al. Biomacromolecules 2009.
[196] Das M, Sanson N, Fava D, Kumacheva E. Langmuir 2007;23:196;
Dong H, Zhu M, Yoon JA, Gao H, Jin R, Matyjaszewski K. J Am Chem Soc 2008;130:12852.
[197] Huang G, Gao J, Hu Z, St. John JV, Ponder BC, Moro D. J Control Release 2004;94:303.
[198] Gao H, Tsarevsky NV, Matyjaszewski K. Macromolecules 2005;38:5995.
[199] Whittaker MR, Goh Y-K, Gemici H, Legge TM, Perrier S, Monteiro MJ. Macromolecules 2006;39:9028.
[200] Wong L, Boyer C, Jia Z, Zareie Hadi M, Davis Thomas P, Bulmus V. Biomacromolecules 2008;9:1934.
[201] Lee Y, Mo H, Koo H, Park J-Y, Cho MY, Jin G-W, et al. Bioconjug Chem 2007;18:13.
[202] Li C, Madsen J, Armes SP, Lewis AL. Angew Chem Int Ed 2006;45:3510.
[203] Zelikin AN, Quinn JF, Caruso F. Biomacromolecules 2006;7:27.
[204] Kakizawa Y, Harada A, Kataoka K. J Am Chem Soc 1999;121:11247.
[205] Kakizawa Y, Harada A, Kataoka K. Biomacromolecules 2001;2:491.
[206] Miyata K, Kakizawa Y, Nishiyama N, Harada A, Yamasaki Y, Koyama H, et al. J Am Chem Soc 2004;126:2355.
[207] Miyata K, Kakizawa Y, Nishiyama N, Yamasaki Y, Watanabe T, Kohara M, et al. J Control Release 2005;109:15.
[208] Li Y, Lokitz BS, Armes SP, McCormick CL. Macromolecules 2006;39:2726.
[209] Zhang L, Liu W, Lin L, Chen D, Stenzel MH. Biomacromolecules 2008;9:3321.
[210] Carelli S, Ceriotti A, Cabibbo A, Fassina G, Ruvo M, Sitia R. Science 1997;277:1681.
[211] Mortell KH, Gingras M, Kiessling LL. J Am Chem Soc 1994;116:12053.
[212] Lu C, Chen X, Xie Z, Lu T, Wang X, Ma J, et al. Biomacromolecules 2006;7:1806.
[213] Mammen M, Chio S-K, Whitesides GM. Angew Chem Int Ed 1998;37:2755.
[214] Bae W-S, Urban MW. Biomacromolecules 2006;7:1156.
[215] Qi K, Ma Q, Remsen EE, Clark Jr CG, Wooley KL. J Am Chem Soc 2004;126:6599.
[216] Gref R, Couvreur P, Barratt G, Mysiakine E. Biomaterials 2003;24:4529.
[217] Costanzo PJ, Patten TE, Seery TAP. Chem Mater 2004;16:1775.
[218] Lai SK, Hida K, Man ST, Chen C, Machamer C, Schroer TA, et al. Biomaterials 2007;28:2876.
[219] Richardson TP, Peters MC, Ennett AB, Mooney DJ. Nat Biotechnol 2001;19:1029.

Jung Kwon Oh received his B.S. and M.S. degrees in Chemistry from Hanyang University, Korea. After over seven years of industrial research experience in emulsion polymerization, he obtained his Ph.D. degree in 2004 at the University of Toronto, Canada with Professor Mitchell A. Winnik in the field of film formation and polymer interdiffusion. He then joined the laboratory of Professor Krzysztof Matyjaszewski at Carnegie Mellon University as a recipient of a prestigious award of a Natural Science and Engineering Research Council (NSERC) Postdoctoral Fellowship of Canada. He developed there inverse miniemulsion atom transfer radical polymerization (ATRP) for synthesis, functionalization, and biomedical application of well-controlled water-soluble/crosslinked nanogels. He is currently employed at Dow Chemical Company in Midland, MI.

Sidi A. Bencherif received two First Class Honors Masters degrees in Physics and Chemistry (2000) and then in Materials and Technology Engineering (2002) from Montpellier II University in France. Sidi came to the United States in 2002 and was employed by the National Institute of Standards and Technology (NIST) as a guest researcher in the Polymer Division. In 2005, he joined the Department of Chemistry at Carnegie Mellon University. His work focused primarily on developing complex degradable synthetic and naturally derived polymeric scaffolds. In 2009, he received a Master of Science degree in Polymer Science and a Ph.D. degree in Chemistry under the supervision of Profs. Matyjaszewski and Washburn. He is currently appointed as a postdoctoral researcher in Matyjaszewski group at Carnegie Mellon. His research interests include: nanogel and star polymer synthesis via controlled radical polymerization techniques, their properties and applications; the development of novel delivery systems; biomacromolecular scaffolds; the controlled delivery of biomolecules; and the design of biomimetic materials to control stem cell fate.

Krzysztof Matyjaszewski was born in Poland in 1950. He obtained his Ph.D. degree in 1976 at the Polish Academy of Sciences in Lodz, Poland, working with Prof. S. Penczek. Since 1985 he has been at Carnegie Mellon University where he is currently J.C. Warner University Professor of Natural Sciences and director of Center for Macromolecular Engineering. His main research interests include controlled/living radical polymerization, catalysis, environmental chemistry, and the synthesis of advanced materials for optoelectronic and biomedical applications. He has co-authored over 600 publications, including 13 monographs and books as well as over 40 US and 100 international patents. His citation record exceeds 30,000 for the last decade and ranks him 3rd in all fields of chemistry. He has formed two industrial consortia focused on controlled radical polymerization at Carnegie Mellon with over 40 international members. He has received doctorate honoris causa from 5 universities, the 2009 Presidential Award in Green Chemistry and several awards from the American Chemical Society, and other institutions. He is a member of US National Academy of Engineering and Polish Academy of Sciences.